agriculture

MDPI

Article

Clove and Lemongrass Essential Oils as Repellents Against *Halyomorpha halys*: From Behavioural Responses to Molecular Interactions and Controlled Release

Ivana Pajač Živković [1], Martina Pajač Beus [1], Helena Viric Gasparic [1,*], Marko Vinceković [2], Kristina Vlahoviček-Kahlina [2], Patrik Tišma [3,4], Višnja Stepanić [3,*] and Darija Lemic [1]

[1] Department of Agricultural Zoology, Faculty of Agriculture, University of Zagreb, Svetošimunska Cesta 25, HR-10000 Zagreb, Croatia; ipajac@agr.hr (I.P.Ž.); mpajacbeu23@student.agr.hr (M.P.B.); dlemic@agr.hr (D.L.)
[2] Department of Chemistry, Faculty of Agriculture, University of Zagreb, Svetošimunska Cesta 25, HR-10000 Zagreb, Croatia; mvincekovic@agr.hr (M.V.)
[3] Ruđer Bošković Institute, Division of Computing and Data Science, Bijenička Cesta 54, HR-10000 Zagreb, Croatia
[4] Department of Chemistry, Faculty of Science, University of Zagreb, Horvatovac 102A, HR-10000 Zagreb, Croatia
* Correspondence: hviric@agr.hr (H.V.G.); visnja.stepanic@irb.hr (V.S.); Tel.: +385-1-239-3804 (H.V.G.)

Abstract

Halyomorpha halys is a highly polyphagous invasive pest whose management still relies heavily on broad-spectrum insecticides, creating a need for more sustainable behaviour-based alternatives. This study evaluated clove leaf and lemongrass essential oils (EOs) as potential repellents against adult *H. halys* by integrating behavioural bioassays, controlled-release formulations, molecular modelling and in silico ecotoxicological assessment. Male and female adults were tested in a two-choice Y-tube olfactometer; the individual EOs were encapsulated in calcium-alginate microspheres, and selected constituents were assessed using molecular docking and computational ecotoxicity models. Clove EO, lemongrass EO and their binary combination induced strong avoidance responses in both sexes, with pooled avoidance ranging from 90.0% to 96.7% and repellency indices from 0.80 to 0.93. No significant differences were detected among the three EO treatments when responses were pooled across sexes ($\chi^2 = 2.14$, $p = 0.343$). Both EOs were successfully incorporated into calcium-alginate microspheres, with encapsulation efficiencies exceeding 90% (91.57 ± 0.67% for clove EO and 96.42 ± 0.29% for lemongrass EO). Lemongrass EO showed higher encapsulation efficiency and loading capacity and reached near-complete cumulative release, whereas clove EO release plateaued at approximately 70%. Phylogenetic, structural and physicochemical analyses supported the selection of *H. halys* HhOBP21 for comparative molecular modelling with the structurally characterised *Drosophila melanogaster* DmOBP28a. Molecular docking indicated that selected EO constituents could be accommodated within the binding cavities of these OBPs, with β-caryophyllene, α-humulene and limonene among the most favourably scored ligands, suggesting potential interactions with these proteins. Predicted acute toxicity values for the standard non-target test organism *Tetrahymena pyriformis*, *Daphnia magna* and *Pimephales promelas* remained below the applied thresholds for all evaluated compounds, although several constituents showed elevated predicted bioconcentration potential and limited biodegradability. Overall, the results demonstrate strong avoidance responses to the tested EOs under laboratory Y-tube conditions and support their further evaluation in semi-field and field studies to determine whether these responses translate into spatial repellency under practical conditions. Experimental validation of predicted molecular interactions and environmental fate is also needed.

Check for updates

Academic Editor: Giacinto S. Germinara

Received: 30 August 2026
Revised: 15 October 2026
Accepted: 26 October 2026
Published: 1 November 2026

Copyright: © 2026 by the authors. Licensee MDPI, Basel, Switzerland. This article is an open access article distributed under the terms and conditions of the Creative Commons Attribution (CC BY) license.

Keywords: brown marmorated stink bug; clove oil; lemongrass oil; behavioural repellency; odorant-binding proteins; molecular docking; controlled release; environmental fate

1. Introduction

Halyomorpha halys (Stål, 1855) is an invasive pentatomid native to East Asia whose economic importance is associated with its broad host range, feeding damage and pronounced dispersal capacity [1–3]. Following its establishment outside its native range, the species has become an important pest of fruit, vegetable, field and ornamental crops in North America and Europe, including agricultural production systems in southeastern Europe [4–6]. More than 300 cultivated and wild plant species have been reported as hosts, while field observations and molecular analyses confirm that *H. halys* feeds on a wide range of woody and herbaceous plants [3,7,8]. The use of multiple cultivated and non-crop hosts allows populations to persist in heterogeneous agricultural landscapes and is associated with seasonal shifts in their spatial distribution [9,10]. Tree fruit production is particularly vulnerable because feeding by nymphs and adults can affect both the external appearance and internal tissue quality of developing fruits, thereby reducing their marketability and, under high pest pressure, marketable yield [6,11]. Feeding injury may manifest as external and internal fruit defects, although its incidence and severity vary among crops, cultivars and fruit developmental stages [4,11,12]. Orchard management is further complicated by seasonal shifts in adult distribution among cultivated and wild hosts, which can lead to continued immigration into production areas and uneven spatial distribution of pest pressure within orchards [9–11].

Management of *H. halys* in commercial crops still relies substantially on repeated applications of broad-spectrum insecticides, including pyrethroids and neonicotinoids, which can cause rapid mortality of exposed individuals [13,14]. However, season-long protection is difficult to achieve because insecticide residues lose efficacy over time and mobile adults continue to immigrate into treated crops [13,15]. Insecticide applications may also expose predators and parasitoids to lethal and sublethal effects, potentially reducing their contribution to biological control [16,17]. Consequently, several alternative management strategies have been evaluated, including physical exclusion with insect-proof netting [18,19], pheromone-based attract-and-kill systems [20,21], biological control with egg parasitoids [22], and insecticidal products derived from natural compounds [23]. Although these approaches can reduce pest abundance or crop injury, their effectiveness may vary depending on crop characteristics, pest pressure, application method and environmental conditions, highlighting the need for complementary measures that interfere with pest behaviour. Volatile plant compounds are therefore promising candidates because they may disrupt host location or elicit avoidance responses in *H. halys*.

Olfactory cues contribute to the orientation of *H. halys* towards conspecifics and host plants. Both adults and nymphs are attracted to the male-produced aggregation pheromone, and this response is enhanced when the pheromone is combined with methyl (E,E,Z)-2,4,6-decatrienoate [24]. Plant-associated odours also influence host-searching behaviour: in Y-tube assays, second-instar nymphs preferred apple and peach odours over clean air and exhibited different responses to the synthetic volatiles tested [25]. Similarly, electrophysiological and Y-tube assays with adults identified linalool oxide as an antennally active plant-derived volatile that attracted *H. halys* at lower and intermediate doses [26]. However, behavioural responses depend on the identity and composition of the odour stimulus, as individual compounds and their blends elicited different patterns of attraction in Y-tube and greenhouse assays [25]. Controlled-choice bioassays are therefore useful for deter-

mining whether a volatile stimulus elicits attraction, avoidance or no directional response. By presenting test and control odour sources simultaneously in separate air streams, a Y-tube olfactometer enables olfactory preference or avoidance to be evaluated without direct contact between the insect and the tested material [25,26].

The practical use of essential oils (EOs) as behaviour-modifying agents depends strongly on their chemical composition and physicochemical properties. Plant EOs are widely investigated as natural crop-protection agents because of their insecticidal, repellent and antimicrobial activities [27,28]. EOs derived from the leaves of clove (*Syzygium aromaticum*) and lemongrass (*Cymbopogon citratus*) contain biologically active volatile constituents, with eugenol generally predominating in clove leaf oil, while citral, a mixture of the two geometric isomers geranial ((E)-citral) and neral ((Z)-citral), constitutes a major fraction of lemongrass oil. These compounds have been associated with insecticidal, repellent and antimicrobial activities, although their efficacy depends on concentration, composition and mode of exposure [29,30]. Previous studies have demonstrated that clove and lemongrass EOs can markedly reduce the response of *H. halys* to attractant-baited traps, while clove oil has also shown repellent activity against adults in controlled laboratory assays [31,32]. Other EOs have also shown effects on *H. halys*: spearmint and ylang-ylang oils reduced responses to attractant-baited traps [31], while turmeric EO showed repellent activity in laboratory assays [32]. Clove and lemongrass EOs were selected because both had shown effects in the same trap-based study [31], providing a rationale for their direct comparison in the present behavioural and formulation analyses. However, the responses of adult *H. halys* to the two oils and their binary combination have not been directly compared under the same assay conditions. It also remains unclear how effectively each oil can be incorporated into a controlled-release carrier and whether selected constituents can interact with *H. halys* odorant-binding proteins. Comparing the individual oils with their blend is important because mixtures of EOs or their constituents may produce behavioural responses that differ from those elicited by the individual components, including additive or synergistic effects reported in other insect systems [33,34]. Behavioural responses of *H. halys* to volatile compounds may also be concentration-dependent, as a compound that is attractive at lower doses may induce avoidance at a higher dose [26].

Despite their promising biological activity, the direct application of EOs in agricultural systems is constrained by several physicochemical properties, including rapid volatilisation, susceptibility to oxidation and light-induced degradation, limited water solubility, and variable persistence under environmental conditions. These characteristics can result in shortened residual activity and variable performance of unformulated EOs [35]. Moreover, poorly controlled local EO concentrations may increase the potential for phytotoxic effects or undesirable exposure of non-target organisms, highlighting the importance of developing delivery systems capable of regulating EO availability [36]. Encapsulation provides a formulation strategy to address these limitations by incorporating EOs into a protective carrier matrix that can reduce their immediate loss, improve physical stability and regulate their release. Previous studies have demonstrated that encapsulation and inclusion complexation can modify EO release characteristics and help preserve their biological activity in formulated systems [37,38]. Biodegradable polymers such as alginate, chitosan and starch have therefore been widely investigated as carrier materials for controlled-delivery systems [39,40]. Among these, alginate is particularly suitable because it forms ionically cross-linked hydrogels in the presence of calcium ions, enabling the incorporation of EOs into microspheres under mild conditions and their subsequent gradual release [41]. The resulting release profile depends on the properties of the polymeric matrix, the incorporated oil and their interactions, all of which may influence the concentration and persistence of biologically active volatiles. In the present study, clove and lemongrass EOs were encapsu-

lated in calcium-alginate microspheres to determine whether these oils could be efficiently incorporated and subsequently released in a controlled manner. Encapsulation efficiency, loading capacity, swelling behaviour and release kinetics were evaluated to characterise the performance of the resulting formulations and to establish a basis for their potential development as EO-based repellent delivery systems.

Because behavioural responses to volatile compounds depend on their detection by the insect olfactory system, odorant-binding proteins (OBPs) provide relevant molecular targets for investigating potential interactions with semiochemicals and EO constituents. OBPs are small soluble proteins involved in the binding, solubilisation and transport of hydrophobic odorants through the aqueous sensillar lymph and thereby contribute to insect chemoreception. Although numerous insect OBPs have been identified, only a subset has been functionally and structurally characterised [42,43]. Their ligand-binding properties and involvement in chemical recognition have consequently attracted increasing interest in their potential use as molecular targets for behaviour-based and targeted pest-management strategies [44]. Molecular docking can provide initial insight into the structural compatibility and predicted interactions between volatile compounds and selected insect OBPs and thus generate hypotheses about possible ligand–OBP interactions [26]. Such molecular recognition may represent an important step in the transport and presentation of semiochemicals to membrane-bound olfactory receptors, although binding to an OBP alone does not establish whether a compound will activate the downstream olfactory signalling pathway or ultimately elicit attraction, repellency or other behavioural responses. Experimental evidence linking ligand–OBP interactions to olfactory function and behaviour is therefore needed to establish the functional significance of predicted binding [45].

The aim of this study was to evaluate the potential of clove leaf and lemongrass EOs as behaviour-modifying agents against adult *H. halys*. Specifically, the study aimed to: (i) compare the olfactory responses of male and female *H. halys* to clove and lemongrass EOs and their binary combination using a Y-tube olfactometer; (ii) characterise the encapsulation performance and release behaviour of the selected EOs in calcium-alginate microspheres; (iii) investigate predicted molecular interactions between selected EO constituents and a selected *H. halys* OBP using molecular docking; and (iv) predict the ecotoxicity and environmental-fate profiles of the selected EO constituents. By integrating behavioural, formulation and computational approaches, the study sought to assess the potential of clove- and lemongrass-based treatments for further development as components of behaviour-based *H. halys* management.

2. Materials and Methods

2.1. Preparation of Microsphere Formulations

Alginic acid sodium salt (CAS number: 9005-38-3, M/G ratio: 1.56, molecular weight: 280,000 g mol^{-1}) was obtained from Sigma-Aldrich (St. Louis, MO, USA). Calcium chloride ($CaCl_2$; CAS number: 10043-52-4; ≥95% purity) was supplied by Kemika (Zagreb, Croatia). Clove leaf essential oil (*Syzygium aromaticum*, labelled as *Eugenia caryophyllata*) was purchased from DEA FLORES d.o.o. (Rijeka, Croatia), and lemongrass essential oil (*Cymbopogon citratus*) was obtained from Pranarôm International S.A. (Ghislenghien, Belgium). Clove and lemongrass EOs were selected as sources of eugenol- and citral-rich oils, respectively [46,47]. The chemical composition of the oils used in this study is reported in Section 2.4.

All other chemicals were of analytical grade and were used without further purification.

The microsphere formulations were prepared according to previously described procedures [48]. For each formulation, 1 mL of clove or lemongrass essential oil was incorporated into a sodium alginate solution to achieve a final volume of 100 mL, corresponding to an EO

concentration of 1% (v/v) and a final sodium alginate concentration of 2% (w/v; 2 g/100 mL). This nominal 1% (v/v) concentration refers to the emulsion before encapsulation and does not represent EO loading per unit mass of microspheres or the EO exposure concentration in the Y-tube assay. The EO–alginate mixture was emulsified using an ultrasonic probe (Hielscher Ultrasonics GmbH, Teltow, Germany) for 2 min in continuous mode at 50% amplitude. Subsequently, 100 mL of the resulting emulsion was added dropwise to 100 mL of a 4% (w/v) calcium chloride ($CaCl_2$) solution using a B-390 encapsulator (BÜCHI Labortechnik AG, Flawil, Switzerland) equipped with a 1000 µm nozzle, operating at a vibration frequency of 40 Hz and an air pressure of 40–60 mbar. The microspheres were maintained in the $CaCl_2$ solution under continuous stirring for an additional 30 min to ensure ionic gelation. The resulting microspheres were then washed with distilled water and stored at 4 °C until further analysis.

2.2. Release of EOs from Microsphere Formulations

The release of clove and lemongrass EOs from microsphere formulations was determined using a UV/VIS spectrophotometer (UV/VIS 1900, Shimadzu, Kyoto, Japan). For the release experiments, 0.2 g of EO-loaded microspheres were dispersed in 100 mL of an aqueous ethanol solution containing 20% (v/v) ethanol (ethanol:distilled water = 20:80, v/v). Absorbance was measured at 282 nm for clove EO and 270 nm for lemongrass EO, corresponding to their respective absorbance maxima. The fraction of released EO (f) was calculated using the following equation:

$$f(\%) = \frac{R_t}{R_{tot}} \times 100$$

where R_t is the amount of EO released at time t, and R_{tot} is the total amount of EO loaded into the microspheres.

The loading capacity (LC) was calculated using the following equation:

$$LC_{EO} = \frac{\gamma_{EO} \times V}{w_c}$$

where γEO is the mass concentration of EO in the sample, V is the sample volume, and wc is the mass of the microsphere formulation.

The encapsulation efficiency (EE) was determined according to the method described by Vinceković et al. [48], based on the initial volumetric concentration of lemongrass or clove EO (Ctot) and the EO content retained in the dry formulations (Cload). Encapsulation efficiency was expressed as a percentage of the initial EO content and calculated using the following equation:

$$EE(\%) = \frac{C_{load}}{C_{tot}} \times 100$$

where $C_{load} = C_{tot} - C_f$, and C_f is the concentration of EO in the filtrate.

To determine the degree of swelling (Sw), dry microparticles (0.1 g) were dispersed in 10 mL of deionised water in a glass vial. The samples were allowed to swell for 3 h at room temperature. After blotting with filter paper to remove surface moisture, the swollen microparticles were immediately weighed to determine their wet mass [49]. The degree of swelling was calculated as a percentage using the following equation:

$$S_w(\%) = \frac{w_t - w_0}{w_0} \times 100$$

where w_t is the mass of the swollen microparticles at time t, and w_0 is the initial dry mass of the microparticles.

2.3. Repellency Bioassay

Adult *H. halys* used in this experiment were collected in September 2025 at the Maksimir Experimental Orchard of the Department of Pomology, University of Zagreb Faculty of Agriculture, using black pyramidal traps baited with an aggregation attractant that attracts both males and females. Based on local phenological monitoring, the collection period corresponded to the emergence of the second adult generation (G2), and the tested insects were therefore considered to belong to the same late-season adult cohort. After collection, insects were transferred to entomological cages and allowed to acclimatise overnight before testing. During this period, they were not provided with additional food. The insects had not previously been experimentally exposed to insecticides. Repellency assays were conducted at the Department of Agricultural Zoology, University of Zagreb Faculty of Agriculture, under controlled laboratory conditions (25 ± 2 °C and 60 ± 10% relative humidity), using a two-choice glass Y-tube olfactometer (Yashika Solutions/Insect Technologies, Madurai, Tamil Nadu, India). The olfactometer was connected via PTFE fittings and silicone tubing to two independently regulated air streams supplied by an external air pump. Airflow was set to 0.5 L min^{-1} in each arm using individual flow meters.

Males and females were tested separately. Insects were allowed to choose between an arm containing EO-loaded calcium-alginate microspheres and an arm containing blank calcium-alginate microspheres as the formulation control. Each assay lasted 5 min. The number of insects selecting the essential-oil arm was recorded as attraction, whereas the number of insects selecting the control arm was recorded as avoidance. Here, "attraction" and "avoidance" are operational terms denoting selection of the EO and control arms, respectively. Preference for the control arm indicates relative avoidance of the EO-loaded microspheres compared with blank calcium-alginate microspheres under the tested two-choice conditions; it does not, on its own, establish spatial repellency under field conditions. All tested individuals made a choice within the 5-min observation period; therefore, no insects were classified as non-responders.

For each treatment–sex combination, three independent replicates were conducted, with 10 insects per replicate, giving a total of 30 males and 30 females per treatment. Ten insects were introduced into the Y-tube simultaneously in each replicate. Individual arm choices were recorded and summarised across the three replicates for each treatment–sex combination. To minimise cross-contamination and carry-over of volatile compounds between treatments, the glass components of the Y-tube olfactometer were washed three times, rinsed with 96% ethanol, and dried completely before reuse. To minimise positional bias, the essential-oil stimulus and the control were switched between the two Y-tube arms between successive replicates. The response was expressed as the percentage of insects choosing each arm.

The percentage of attraction was calculated as:

$$A(\%) = \frac{N_{EO}}{N_{resp}} \times 100$$

The percentage of avoidance was calculated as:

$$Av(\%) = \frac{N_{C}}{N_{resp}} \times 100$$

where N_{EO} is the number of insects choosing the essential-oil arm, N_{C} is the number of insects choosing the control arm, and N_{resp} is the total number of responding insects.

To quantify the strength and direction of the behavioural response, a repellency index (RI) was calculated for each treatment–sex combination using the following equation:

$$RI = \frac{N_{C} - N_{EO}}{N_{resp}}$$

where *N*C is the number of insects choosing the control arm, *N*EO is the number of insects choosing the essential-oil arm, and *N*resp is the total number of responding insects (*N*resp = *N*C + *N*EO). The RI ranges from −1 to +1, with positive values indicating avoidance of the essential-oil stimulus, values close to zero indicating no clear preference, and negative values indicating attraction to the essential-oil stimulus.

The observed distribution of insects between the essential-oil arm and the control arm was compared with the expected 1:1 distribution using a chi-square goodness-of-fit test. This test was applied separately for each treatment–sex combination to determine whether the observed response differed significantly from random choice. In addition, data were pooled across sexes to compare the overall behavioural responses among essential-oil treatments. For each treatment, the numbers of insects choosing the essential-oil and control arms were summed across males and females and expressed as percentages, and the corresponding repellency index was calculated. Differences in the distribution of attraction and avoidance responses among treatments were tested using a chi-square test of independence. All data processing and statistical analyses were performed using ARM software (revision 2025.2; Gylling Data Management Inc., Brookings, SD, USA) [50].

2.4. Gas Chromatography–Mass Spectrometry (GC-MS) Analysis

The clove leaf and lemongrass essential oils used in the present study were diluted in n-hexane by mixing 10 µL of each EO with 1000 µL of solvent, and their chemical compositions were analysed using a Shimadzu GC-2030/QP2020 NX GC–MS system (Shimadzu Corporation, Kyoto, Japan) equipped with an SH-I-5Sil MS fused-silica capillary column (30 m × 0.25 mm i.d.; film thickness, 0.25 µm) and an electron ionisation (EI) mass spectrometer.

The injection volume was 1 µL, with a split ratio of 50:1 and an inlet temperature of 250 °C. Helium was used as the carrier gas at a flow rate of 1.0 mL/min. The solvent delay was 2.5 min, the mass scan range was m/z 40–400, the EI source temperature was 230 °C, and the electron ionisation energy was 70 eV. The oven temperature was initially set at 60 °C for 1 min, then increased at 3 °C/min to 200 °C and held for 10 min, resulting in a total run time of approximately 57.7 min. Data acquisition and processing were performed using GCMSsolution software (Shimadzu Corporation, Kyoto, Japan).

Compounds were tentatively identified by comparing their mass spectra with reference spectra from the NIST/EPA/NIH Mass Spectral Library 2020. The relative abundance of each component was calculated from its peak area as a percentage of the total integrated peak area (Area%). The retention times (tR) of the identified compounds were also recorded and are provided together with the corresponding mass spectra in the Supplementary Materials.

2.5. In Silico Analyses

2.5.1. Ligand Selection and Preparation

Selected representative constituents of clove leaf and lemongrass EOs were identified based on information provided in the corresponding Safety Data Sheets (SDSs) for inclusion in the in silico analyses (Figure 1). To support the selection of these compounds, GC–MS analyses of the EOs used in this study were carried out (Section 2.4). The GC–MS results largely confirmed the presence of the selected constituents (Section 3.4), with the corresponding chromatographic profiles and mass spectra provided in the Supplementary Materials.

The corresponding SMILES representations were retrieved from the PubChem database [51]. Three-dimensional structures and relevant stereoisomeric forms of the selected compounds were generated and prepared using LigPrep (Schrödinger Release 2026-2) with default settings [52]. The two biologically active stereoisomers of the *H. halys*

aggregation pheromone murgantiol, (3S,6S,7R,10S)- and (3R,6S,7R,10S)-10,11-epoxy-1-bisabolen-3-ol, were included as reference ligands and prepared using the same procedure.

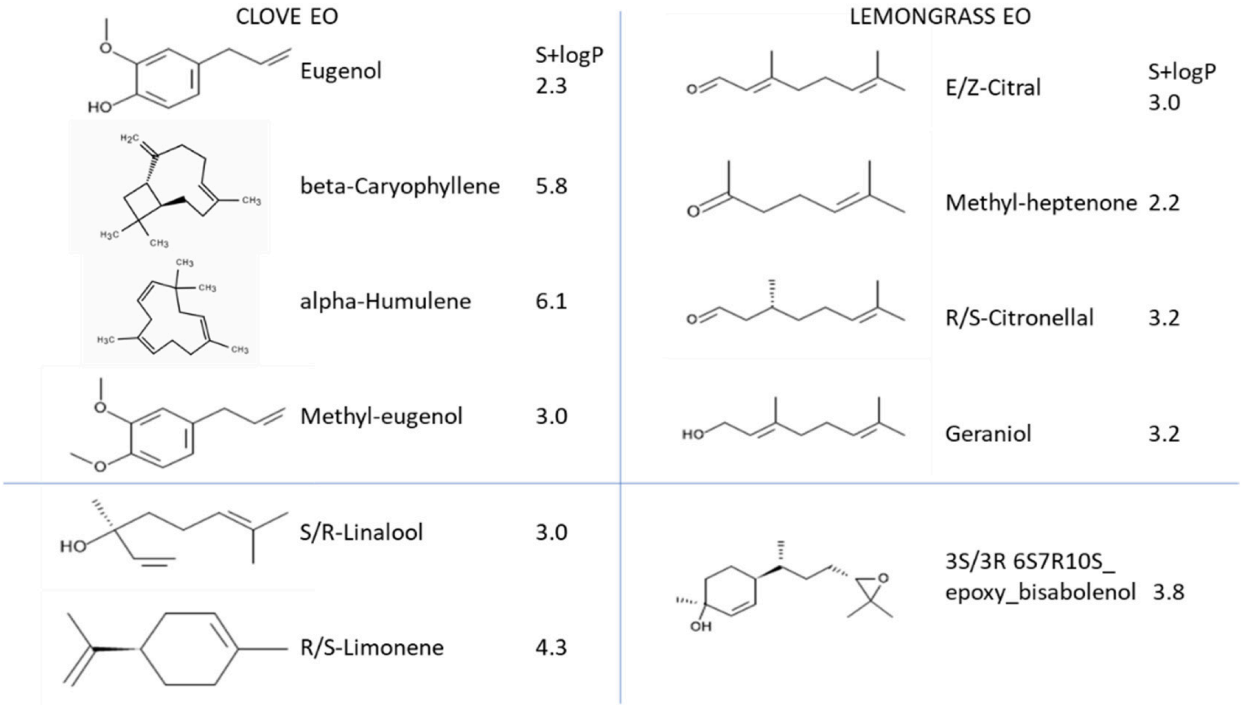


Figure 1. Chemical structures of selected constituents reported for clove and lemongrass EOs and included in the in silico analyses, together with the two biologically active stereoisomers of the *H. halys* aggregation pheromone, (3S,6S,7R,10S)- and (3R,6S,7R,10S)-10,11-epoxy-1-bisabolen-3-ol [53]. For molecular docking, both stereoisomers (E/Z or R/S, as applicable) were included for linalool, limonene, citral, and citronellal. The other compounds were used in the forms shown. The n-octanol/water partition coefficients (S+logP) calculated using ADMET Predictor™ are also shown.

2.5.2. Odorant-Binding Proteins (OBPs)

Because no experimentally determined structures of *H. halys* OBPs were available, OBPs from *Drosophila melanogaster* were included as a comparative reference set to support the selection and structural evaluation of a suitable *H. halys* OBP for molecular modelling. *D. melanogaster* was not considered a target species of the present study. Rather, its OBPs were used because they are comparatively well characterised and an experimentally determined X-ray crystal structure is available for DmOBP28a (PDB ID: 6QQ4) [45]. This experimentally resolved structure served as a reference for evaluating the phylogenetic relationships, three-dimensional similarity and physicochemical characteristics of the *H. halys* OBPs.

The amino acid sequences in FASTA format of 30 unreviewed *H. halys* odorant-binding proteins (HhOBPs) and 20 reviewed *D. melanogaster* odorant-binding proteins (DmOBPs) were retrieved in FASTA format from UniProtKB in July 2025. The *H. halys* sequences corresponded to unreviewed UniProtKB/TrEMBL entries, whereas the *D. melanogaster* sequences corresponded to reviewed UniProtKB/Swiss-Prot entries. The retrieved sequences were compared in terms of sequence characteristics, phylogenetic relationships, structural similarity and physicochemical properties. This comparative analysis was used to identify an *H. halys* OBP showing the strongest overall correspondence to a structurally characterised reference OBP and therefore considered suitable for subsequent ligand-binding analyses [54].

Three-dimensional structures of the selected OBPs were obtained from the AlphaFold Protein Structure Database [55,56] and used for subsequent molecular modelling of OBP–

ligand complexes. The experimentally determined crystal structure of DmOBP28a (PDB ID: 6QQ4) was retrieved from the Protein Data Bank (PDB) and included as a reference for comparison with the predicted OBP models [45].

2.5.3. Sequence, Phylogenetic, Structural and Physicochemical Analyses of OBPs

Multiple sequence alignments (MSAs) of OBP amino acid sequences were generated using the ClustalW algorithm in MEGA 11 and visualised using Jalview version 2.11.5.2 [57,58]. Regions containing a high proportion of gaps were trimmed prior to phylogenetic analysis to exclude poorly aligned positions that could reduce the reliability of phylogenetic inference.

Following refinement of the MSAs, phylogenetic analyses were performed using IQ-TREE [59]. ModelFinder Plus (MFP) was used to determine the best-fit amino acid substitution model [60]. The best-fit model was selected according to the model-selection criterion implemented in IQ-TREE. Maximum-likelihood trees were inferred using 1000 ultrafast bootstrap replicates to assess branch support [61]. The resulting phylogenetic tree was visualised and annotated using FigTree version 1.4.4 [62]. The Foldseek Search Server was also used to assess three-dimensional structural similarities and identify potential structural homologues among OBPs from the two insect species [63].

Physicochemical properties, including molecular weight (MW), theoretical isoelectric point (pI), grand average of hydropathicity (GRAVY), sequence length and amino acid composition (%), were calculated using the ProtParam module implemented in the Biopython library [64]. Principal component analysis (PCA) was subsequently performed using DataWarrior [65] to explore clustering patterns based on these physicochemical properties and sequence-derived features.

2.5.4. Molecular Modelling of Selected OBP–Ligand Complexes

Molecular modelling of complexes formed between the selected OBPs and EO constituents was performed using Glide molecular docking software (Schrödinger Release 2026-2) [52].

Docking calculations included three receptor structures: the experimentally determined crystal structure of DmOBP28a (PDB ID: 6QQ4), the AlphaFold-predicted structure of DmOBP28a (AF-P54195), and the predicted structure of the selected *H. halys* protein HhOBP21 (AF-A0A1L2JGT1). For the crystal structure, docking was performed at the pentaethylene glycol (1PE)-binding site of chain A, whereas for the AlphaFold-predicted structures, putative ligand-binding sites were identified using the SiteMap module (Schrödinger Release 2026-2) [52,56].

Receptor grids were centred at the centroids of the selected amino acid residues defining the putative binding sites, which were characterised by SiteScore and DScore values greater than 1 [66]. Water molecules present in the 6QQ4 crystal structure were removed prior to docking.

Molecular docking was performed using the Standard Precision (SP) mode in Glide (Schrödinger Release 2026-2) [52]. A maximum of three binding poses was retained for each ligand, and post-docking energy minimisation was performed for all reported poses.

2.5.5. Computational Ecotoxicological Assessment

Ecotoxicity and environmental-fate properties of the selected EO constituents were predicted using artificial neural network (ANN) models implemented in ADMET Predictor™ version 11 for standard acute ecotoxicity endpoints, bioconcentration and biodegradability [67]. The predicted acute toxicity endpoints for *Pimephales promelas* (fathead minnow), *Daphnia magna* and *Tetrahymena pyriformis* were included to provide a screening-level as-

sessment of the potential ecotoxicity of the investigated EO constituents towards non-target organisms. These species are established model organisms in ecotoxicological assessment and were not selected as taxonomic or physiological surrogates for *H. halys* [68].

Ecotoxicity was evaluated using three acute toxicity endpoints for *Tetrahymena pyriformis*, *Daphnia magna* and *Pimephales promelas*. Toxicity to *T. pyriformis* was expressed as $pIGC_{50}$, defined as the negative logarithm of the concentration causing 50% growth inhibition after approximately 40 h of exposure, with IGC_{50} expressed in mmol/L. Acute toxicity to *D. magna* and *P. promelas* was predicted as LC_{50} (mg/L) after 48 and 96 h of exposure, respectively. For comparison and classification, the predicted LC_{50} values for *D. magna* and *P. promelas* were converted from mg/L to mol/L and expressed as pLC_{50} values, defined as $-\log_{10}(LC_{50}\ [\text{mol/L}])$.

Toxicity thresholds were selected based on the regression plots provided in the ADMET Predictor™ version 11 documentation. For the purposes of the present comparative assessment, compounds with predicted values of $pIGC_{50} \geq 2$ for *T. pyriformis* and $pLC_{50} \geq 7$ for *D. magna* and *P. promelas* were classified as meeting or exceeding the applied toxicity thresholds.

Bioaccumulation potential was assessed using the Bioconcn endpoint, corresponding to the predicted bioconcentration factor (BCF), defined as the ratio of the chemical concentration in fish to that in the surrounding water. For the purposes of the present analysis, a Bioconcn value ≥ 25 was used as the threshold. Environmental biodegradability was assessed using the ANN-based Biodegradn classification model, which predicts the likelihood of biodegradation based on biological oxygen demand. In addition, the predicted *n*-octanol/water partition coefficient (S+logP) was used as an indicator of compound lipophilicity (Figure 1).

3. Results

3.1. In Vitro Release of EOs from Calcium-Alginate Microspheres

The release profiles of clove and lemongrass EOs from calcium-alginate microspheres are presented in Figure 2. Both formulations exhibited biphasic release kinetics, with an initial rapid release phase followed by a slower sustained-release phase until equilibrium was reached. Lemongrass EO showed grater cumulative release, reaching approximately 95–100%, whereas clove EO plateaued at approximately 70%.

The release data for the initial stage (corresponding to the first approximately 60% of EO released) were fitted to the Korsmeyer–Peppas (KP) model [69]: where k is the kinetic constant and n is the release exponent.

The initial portion of the release profiles, corresponding to approximately the first 60% of EO released, was fitted to the Korsmeyer–Peppas model. The model provided good fits for both formulations, with R^2 values of 0.9755 and 0.9953 for clove and lemongrass EO, respectively. The estimated release exponent (n) was 0.183 for ALG/Ca/Clove EO and 0.399 for ALG/Ca/Lemongrass EO, while the corresponding kinetic constants (k) were 29.06 and 14.31 h^{-n}, respectively (Table 1). Because the model was applied only to the initial release phase, these parameters were used for comparative characterisation of early-stage release behaviour rather than for definitive assignment of the overall release mechanism.

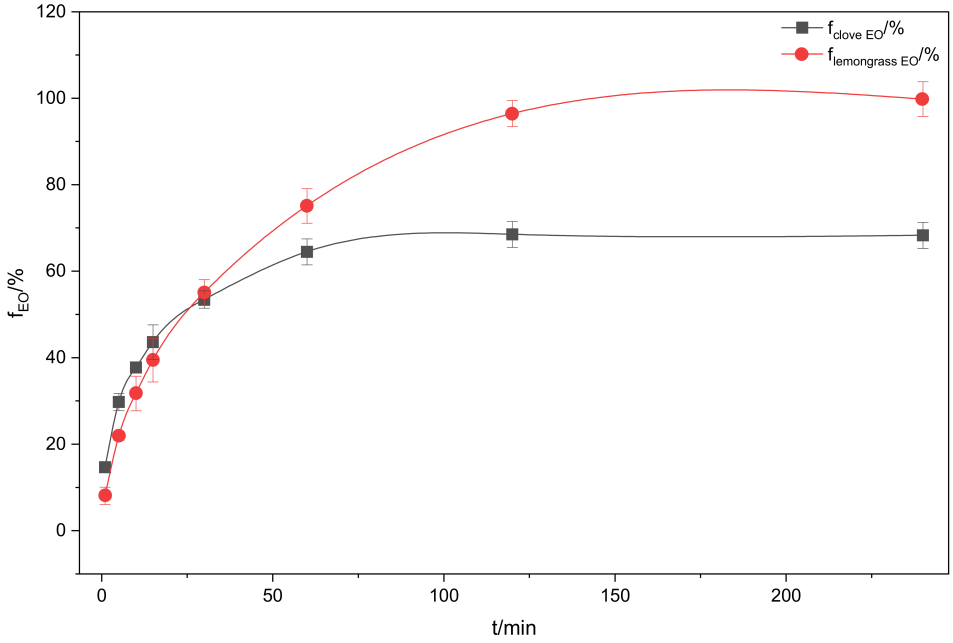


Figure 2. Cumulative release of clove and lemongrass EOs from calcium-alginate microspheres over time. Release is expressed as a percentage of the total EO content. Data are presented as the mean ± standard deviation.

Table 1. Release kinetic parameters of clove- and lemongrass-EO-loaded microspheres in an ethanol/distilled water mixture (20% ethanol, *v*/*v*) at 25 °C, determined using the Korsmeyer–Peppas model. *k* is the kinetic constant (h^{-n}), *n* is the release exponent, and R^2 is the coefficient of determination.

Microsphere Formulations	k/h^n	n	R^2
ALG/Ca/Clove EO	29.06	0.183	0.9755
ALG/Ca/Lemongrass EO	14.31	0.399	0.9953

3.2. Encapsulation Efficiency, Loading Capacity and Swelling Behaviour

The encapsulation efficiency (EE), loading capacity (LC), and degree of swelling (Sw) of calcium-alginate microspheres are presented in Table 2.

Table 2. Encapsulation efficiency (EE), loading capacity (LC), and degree of swelling (Sw) of calcium-alginate microspheres loaded with clove or lemongrass EO.

Microsphere 1.	EE/%	LC/μL g^{-1}	S_w/%
ALG/Ca/Lemongrass EO	96.42 ± 0.29	8.77 ± 0.14	35.17 ± 1.39
ALG/Ca/Clove EO	91.57 ± 0.67	7.06 ± 0.02	38.23 ± 1.41

Both formulations exhibited high encapsulation efficiencies (>90%). ALG/Ca/Lemongrass EO exhibited higher EE (96.42 ± 0.29%) than ALG/Ca/Clove EO (91.57 ± 0.67%). Similarly, the loading capacity was higher for ALG/Ca/Lemongrass EO (8.77 ± 0.14 μL g^{-1}) than for ALG/Ca/Clove EO (7.06 ± 0.02 μL g^{-1}).

The degree of swelling was comparable between the two formulations. ALG/Ca/Clove EO showed a slightly higher degree of swelling (38.23 ± 1.41%) than ALG/Ca/Lemongrass EO (35.17 ± 1.39%).

3.3. Repellency Responses to EO Treatments

Across all tested treatments, the majority of insects selected the control arm, indicating a strong avoidance response to the tested essential-oil stimuli. Avoidance ranged from 86.7% in females exposed to clove EO to 100% in females exposed to lemongrass EO (Figure 3). In males, avoidance was 93.3% for all three treatments (28/30; 95% CI: 78.7–98.2%). Among females, avoidance was 86.7% for clove EO (26/30; 95% CI: 70.3–94.7%), 100% for lemongrass EO (30/30; 95% CI: 88.6–100.0%), and 93.3% for the clove + lemongrass treatment (28/30; 95% CI: 78.7–98.2%).

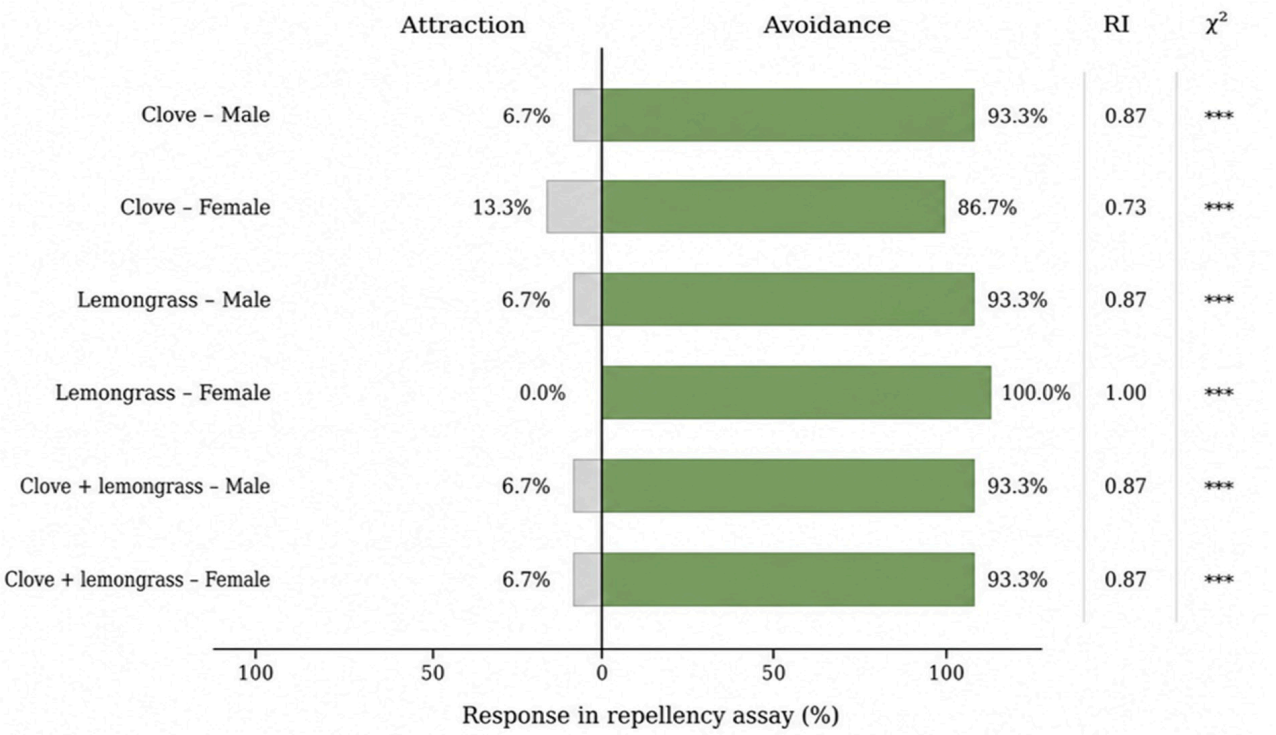


Figure 3. Attraction and avoidance responses of adult *H. halys* to selected essential-oil treatments in a two-choice Y-tube assay. RI: repellency index; ***: significant deviation from the expected 1:1 distribution according to the chi-square goodness-of-fit test ($p < 0.001$).

The repellency index was positive for all treatment–sex combinations, ranging from 0.73 to 1.00, indicating a consistent preference for the control arm over the EO-treated arm. The highest observed avoidance was recorded in females exposed to lemongrass EO, with none of the 30 tested individuals selecting the EO arm (RI = 1.00). Sex effects and treatment × sex interactions were not tested. In all tested combinations, the observed distribution of insects differed significantly from the expected 1:1 ratio, indicating that the responses deviated significantly from an equal distribution (χ^2 tests, $p < 0.001$).

When data were pooled across sexes, all essential-oil treatments elicited a strong avoidance response, with avoidance ranging from 90.0% for clove EO to 96.7% for lemongrass EO. The repellency index was positive for all treatments and ranged from 0.80 to 0.93. However, the distribution of attraction and avoidance responses did not differ significantly among the tested essential-oil treatments ($\chi^2 = 2.14$, df = 2, $p = 0.343$).

3.4. Chemical Composition of Essential Oils (GC–MS Analysis)

Eugenol (76.45%) and β-caryophyllene (14.89%) were the predominant constituents of clove leaf EO, while α-humulene (5.05%) and 15-hydroxy β-caryophyllene (3.60%) were identified as additional constituents. Lemongrass EO was dominated by citral, com-

prising the isomeric aldehydes geranial (41.32%) and neral (27.20%). Other identified constituents included geraniol (5.92%), neryl acetate ((2Z)-3,7-dimethylocta-2,6-dien-1-yl acetate; 5.82%) and methyl heptanone (3.22%), while linalool was present as a minor component (1.90%). The corresponding chromatographic profiles and mass spectra are provided in the Supplementary Materials.

3.5. In Silico Analyses

3.5.1. Bioinformatic Characterisation and Selection of OBPs

The 30 HhOBPs were compared with 20 OBPs from the well-characterised reference species D. melanogaster (DmOBPs) based on their sequence characteristics, phylogenetic relationships, structural features and physicochemical properties. Multiple sequence alignment revealed a characteristic pattern of six conserved cysteine residues in 48 of the 50 analysed OBPs (96%) (Figure 4). Only DmOBP5 (UniProt ID: P54185) and DmOBP10 (UniProt ID: Q27377) did not exhibit this pattern. The conserved cysteines followed the characteristic spacing pattern C–X_{25}–C–X_3–C–X_{36}–C–X_8–C–X_8–C.

Despite the conservation of these cysteine residues, substantial overall sequence divergence was observed. Within the HhOBP set, the median pairwise sequence identity was 18%, whereas the highest sequence identity (72%) was observed between HhOBP7 and HhOBP10. Among DmOBPs, the median pairwise sequence identity was 16%, with DmOBP57a and DmOBP57b showing the highest identity (51%). Pairwise comparisons between HhOBPs and DmOBPs yielded a median sequence identity of 16%.

Phylogenetic analysis identified both predominantly species-specific groups and several clades containing OBPs from both species. The clade highlighted in Figure 4 contained DmOBP19d and DmOBP28a together with seven HhOBPs. Because an experimentally determined crystal structure is available for DmOBP28a (PDB ID: 6QQ4), this protein was selected as the reference OBP for subsequent structural comparisons.

Structural comparison of the seven candidate HhOBPs belonging to this phylogenetic group with DmOBP28a using the Foldseek Search Server revealed that HhOBP21 had the highest structural similarity to the DmOBP28a crystal structure (PDB ID: 6QQ4, chain A), with an E-value of 5.24×10^{-16} and a sequence identity of 30.6%. The structural alignment covered residues 2–121 of HhOBP21. When the AlphaFold model of DmOBP28a (AF-P54195) was used as the reference structure, HhOBP21 yielded an E-value of 1.38×10^{-18}.

PCA based on physicochemical properties and amino acid composition showed that DmOBP28a and HhOBP21 were positioned close together in the PCA score plot, while the loading plot indicated the variables contributing most strongly to the observed separation among OBPs (Figure 5). The mean theoretical pI values were 5.73 for DmOBPs and 6.22 for HhOBPs. Most OBPs from both species exhibited slightly negative GRAVY values, with an overall mean of approximately −0.30. Aspartate (D), glutamate (E), lysine (K), alanine (A), leucine (L) and glycine (G) each accounted for more than 6% of the amino acid composition of both DmOBP28a and HhOBP21.

The combined phylogenetic, structural and physicochemical analyses supported the putative function of HhOBP21 as an OBP, which was subsequently selected for molecular modelling alongside the reference protein DmOBP28a.

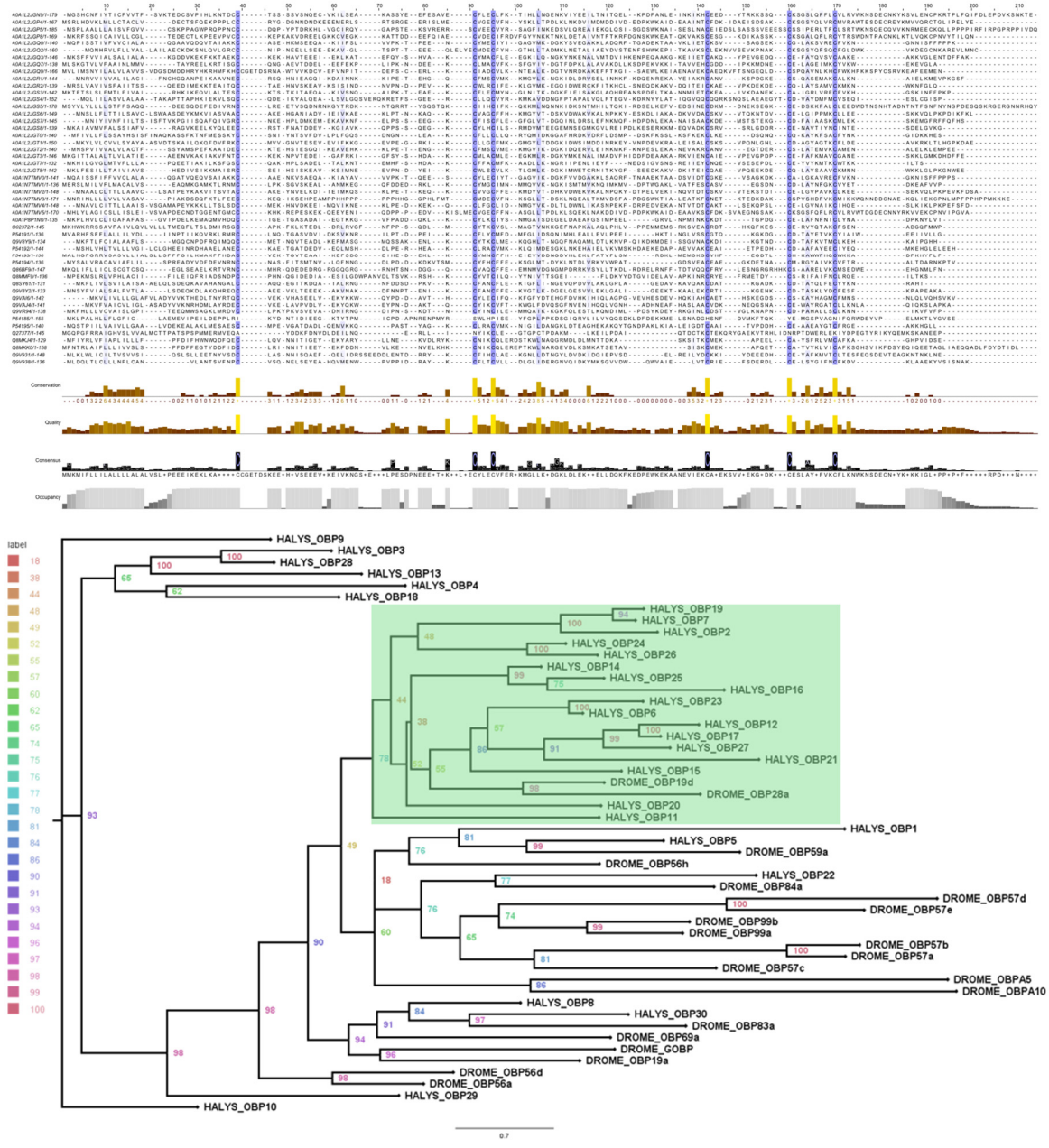


Figure 4. Upper panel: conserved regions of the MSA of 30 HhOBPs and 20 DmOBPs. Sequence identifiers correspond to the respective AlphaFold or UniProt accession numbers. Lower panel: maximum-likelihood phylogenetic tree of OBPs from *H. halys* and *D. melanogaster*, inferred using IQ-TREE with the VT+F+R5 substitution model and 1000 ultrafast bootstrap replicates. The clade containing DmOBP19d, DmOBP28a and seven HhOBPs is highlighted.

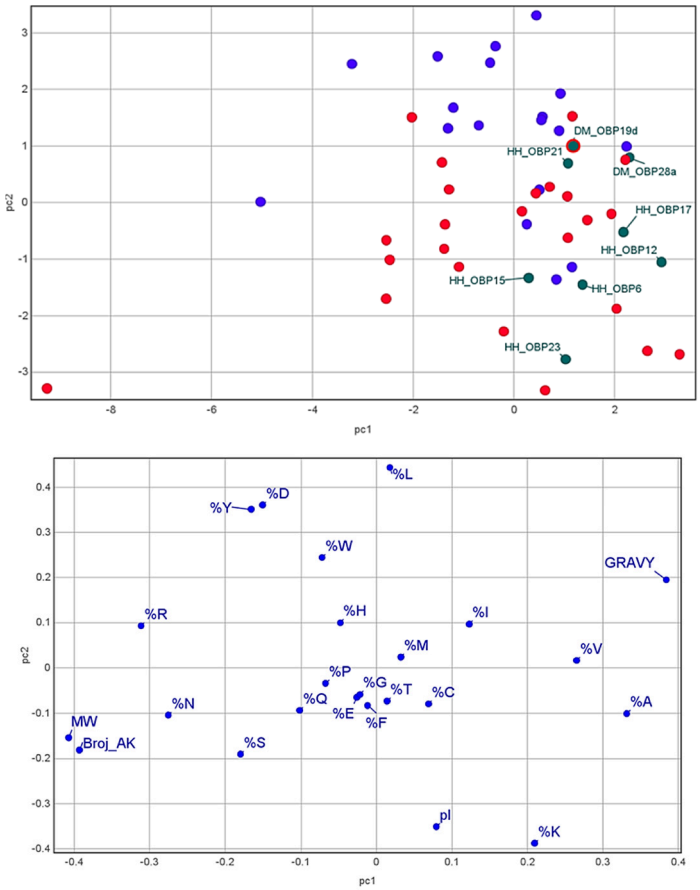


Figure 5. PCA score and loading plots based on the physicochemical properties and amino acid composition of 50 OBPs, comprising 30 HhOBPs (red) and 20 DmOBPs (blue). PC1 and PC2 explained 19.6% and 11.1% of the total variance, respectively. OBPs belonging to the clade highlighted in Figure 4 are labelled.

3.5.2. Molecular Docking of Selected OBPs with EO Constituents

The potential binding of the studied EO constituents to HhOBP21 and the reference protein DmOBP28a was investigated using Glide molecular docking. Docking calculations were performed using the AlphaFold structures of HhOBP21 and DmOBP28a, together with the experimentally determined crystal structure of DmOBP28a (PDB ID: 6QQ4).

The Glide GScore values obtained for the studied clove and lemongrass EO constituents and the two biologically active stereoisomers of the *H. halys* aggregation pheromone are presented in Figure 6. Although the absolute GScore values differed among the three receptor structures, the scores obtained using the different structures were strongly correlated, with Pearson correlation coefficients ranging from 0.854 to 0.873.

The most favourably scored ligands included β-caryophyllene, α-humulene and limonene. The two aggregation-pheromone stereoisomers also showed relatively low GScore values for the investigated OBPs. The predicted binding poses indicated that the studied ligands could be accommodated within the selected binding cavities, although their orientations and interactions with individual amino acid residues varied across ligands and receptor structures.

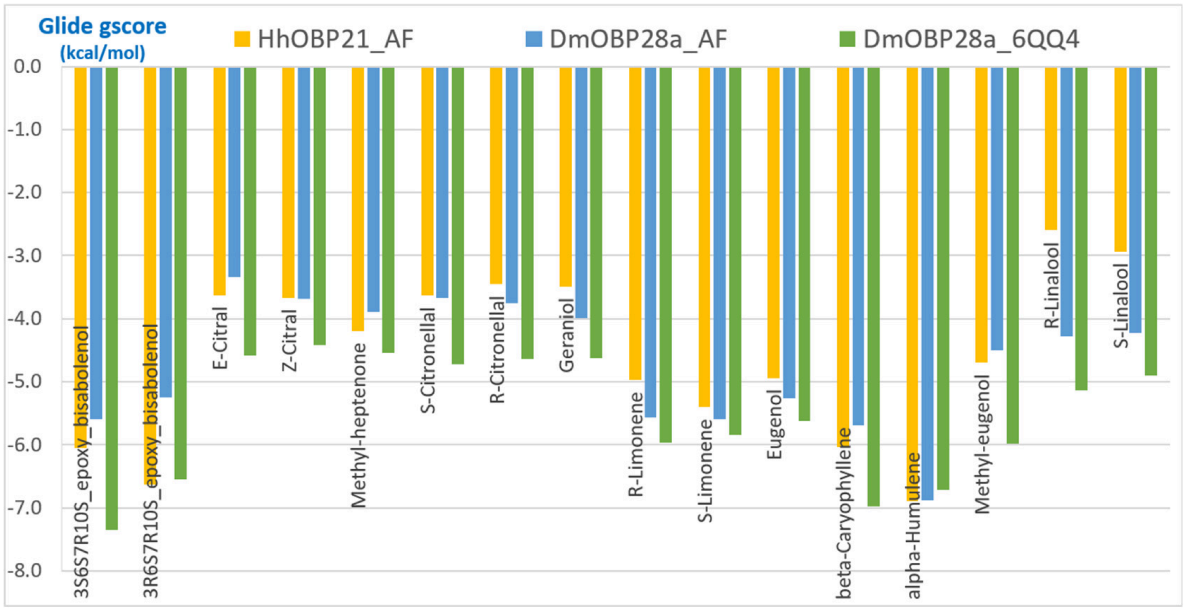


Figure 6. Glide GScore values obtained from molecular docking of clove and lemongrass EO constituents and the two biologically active stereoisomers of the *H. halys* aggregation pheromone with the AlphaFold structures of HhOBP21 and DmOBP28a and the reference crystal structure of DmOBP28a (PDB ID: 6QQ4). More negative GScore values indicate more favourable predicted ligand–protein interactions.

For HhOBP21, the investigated ligands occupied the binding region identified in the AlphaFold structure using SiteMap. For DmOBP28a, the predicted ligand positions differed between the crystal and AlphaFold structures. In the crystal structure (6QQ4), docking was performed within the experimentally observed pentaethylene glycol-binding region, whereas the SiteMap-predicted binding site was used for the AlphaFold structure.

Representative docking poses of the most favourably scored ligands in HhOBP21 and DmOBP28a (Figure 6) are shown in Figures 7 and 8, illustrating their accommodation within the selected OBP binding cavities and their main predicted binding interactions.

3.5.3. Predicted Ecotoxicity and Environmental Fate of EO Constituents

The predicted ecotoxicity and environmental-fate profiles of the selected clove and lemongrass EO constituents are presented in Figure 9. For all investigated compounds, the predicted acute toxicity values for *Tetrahymena pyriformis*, *Daphnia magna* and *Pimephales promelas* remained below the applied thresholds.

Bioconcn values exceeding the applied threshold were predicted for six compounds: β-caryophyllene, α-humulene, limonene, methyl eugenol, linalool and geraniol. β-Caryophyllene, α-humulene and methyl eugenol were also predicted not to be readily biodegradable.

Overall, the predicted profiles revealed more pronounced differences among compounds in bioaccumulation potential and biodegradability than in acute toxicity towards the three aquatic test organisms.

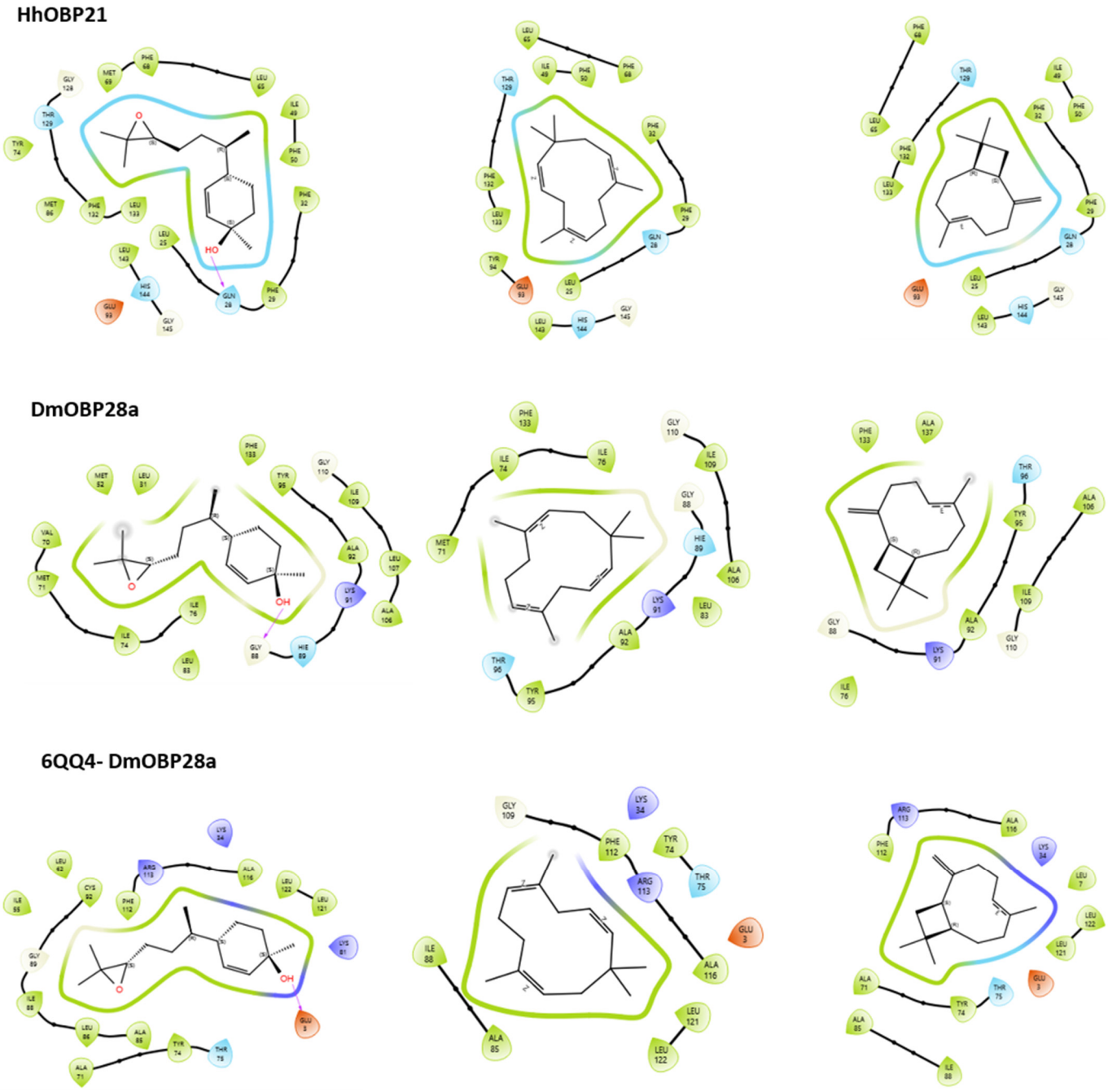


Figure 7. Two-dimensional interaction diagrams showing representative docking poses of the most favourably scored ligands: the (3S,6S,7R,10S) stereoisomer of murgantiol (**left**), α-humulene (**middle**) and β-caryophyllene (**right**) in HhOBP21 and DmOBP28a. The binding site in the DmOBP28a crystal structure (6QQ4) was defined by the co-crystallised pentaethylene glycol ligand, whereas the binding sites in the AlphaFold models were predicted using SiteMap. Hydrophobic, polar, cationic and anionic amino acid residues are coloured green, cyan, blue-violet and orange, respectively. The contour around each ligand indicates solvent exposure, ranging from green (buried) through cyan (partially exposed) to dark blue/purple (highly solvent-exposed).

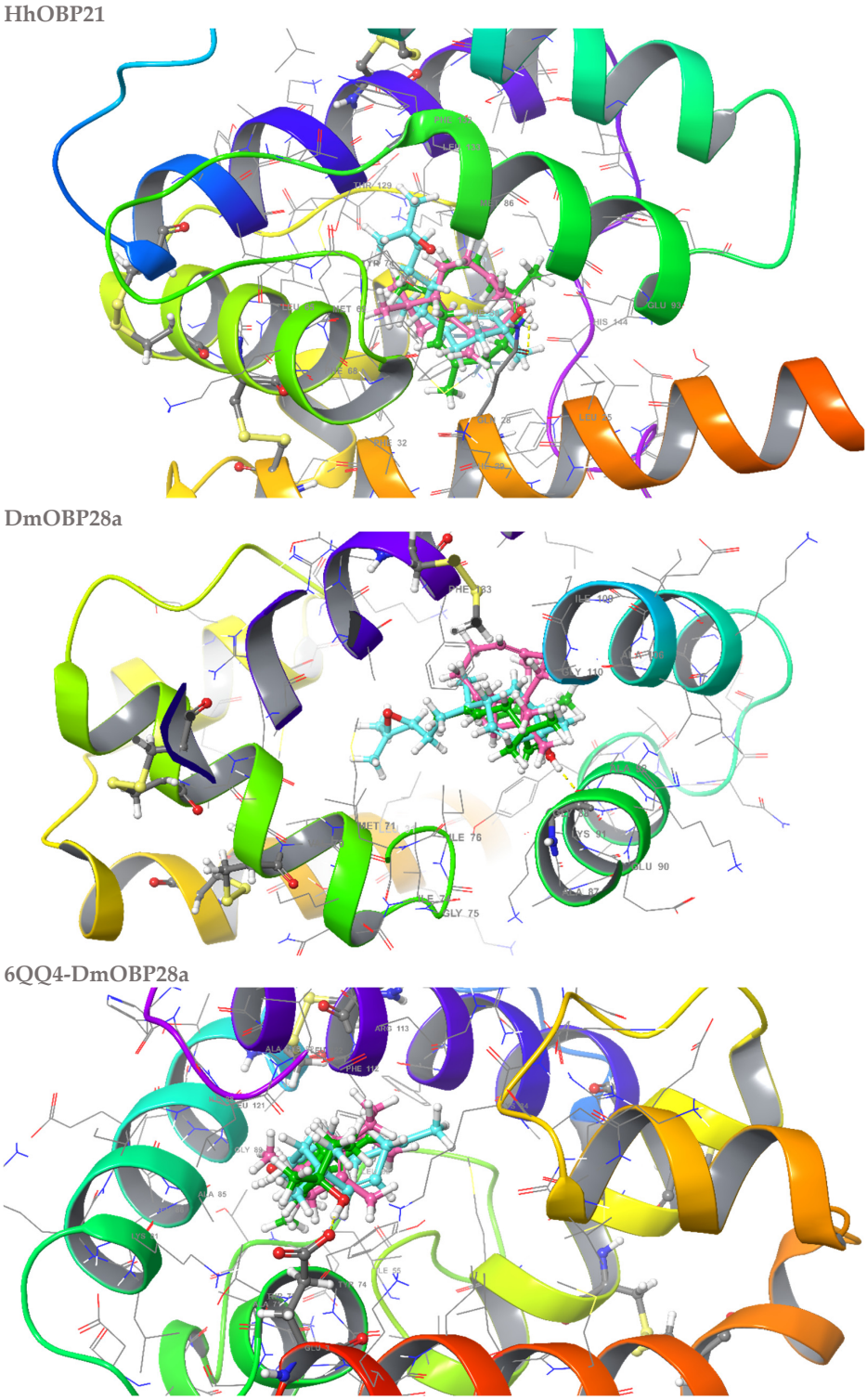


Figure 8. Three-dimensional representations of the docking poses of the most favourably scored ligands within the binding sites of HhOBP21 and DmOBP28a: the (3S,6S,7R,10S) stereoisomer of murgantiol (cyan), α-humulene (green) and β-caryophyllene (pink). The free hydroxyl group of murgantiol forms a hydrogen bond with the side-chain amide group of Gln28, the backbone carbonyl group of Gly88, and the side-chain carboxylate group of Glu3 in HhOBP21, the AlphaFold model of DmOBP28a, and the DmOBP28a crystal structure (6QQ4), respectively. These residues and the disulfide bridges are shown in stick representation.

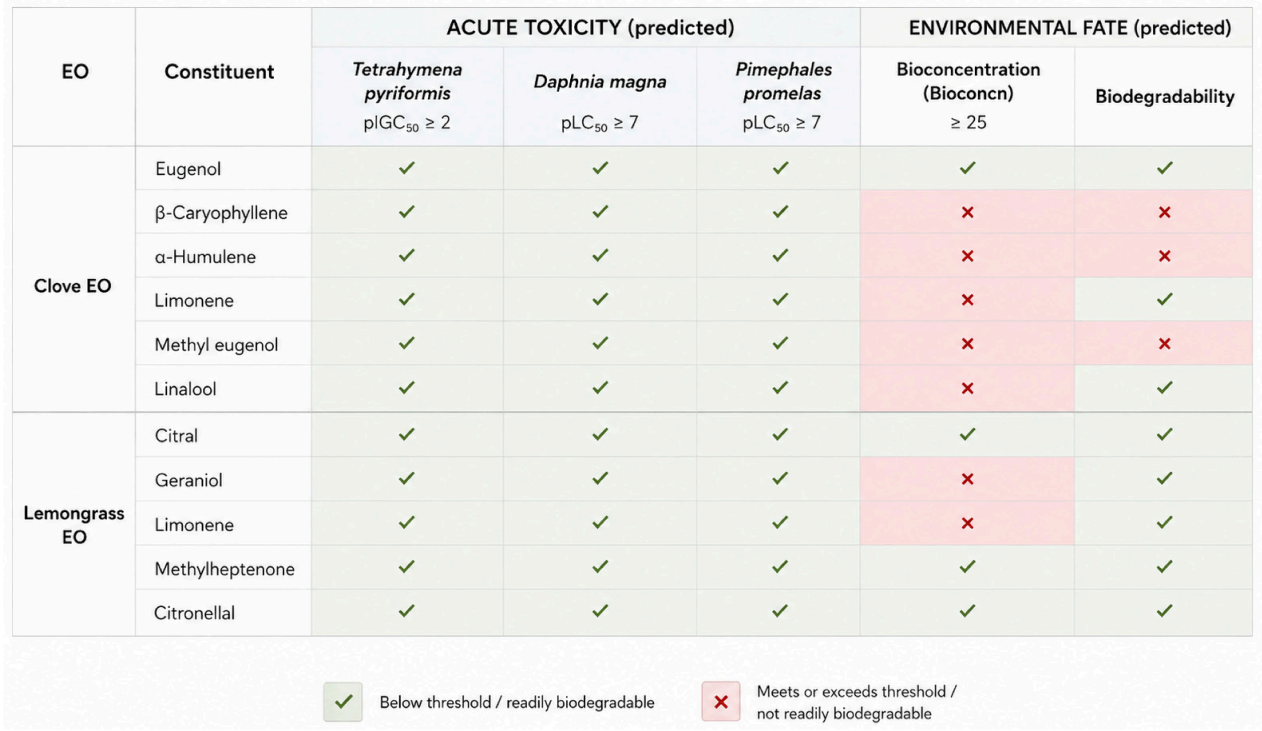


Figure 9. Predicted ecotoxicity and environmental-fate profiles of selected constituents of clove and lemongrass EOs. Acute toxicity was predicted for *Pimephales promelas*, *Tetrahymena pyriformis* and *Daphnia magna*. Green indicates predicted values below the applied toxicity or Bioconcn thresholds and compounds predicted to be readily biodegradable, whereas red indicates values meeting or exceeding the applied thresholds or compounds predicted not to be readily biodegradable. The applied thresholds were $pLC_{50} \geq 7$ for *P. promelas* and *D. magna*, $pIGC_{50} \geq 2$ for *T. pyriformis*, and Bioconcn ≥ 25.

4. Discussion

4.1. Repellent Activity of Clove and Lemongrass EOs

The present study demonstrated a consistent preference for blank microspheres over microspheres loaded with clove or lemongrass EO in adult *H. halys* under controlled Y-tube conditions. All treatments elicited pronounced avoidance of the treated odour source, with pooled avoidance ranging from 90.0% to 96.7% and repellency indices from 0.80 to 0.93. These results are consistent with previous studies showing that clove and lemongrass EOs can interfere with the orientation of *H. halys* and reduce its response to attractant-baited traps [31]. Repellent activity of clove EO against adults has also been demonstrated under controlled laboratory conditions, although the response may vary with the physiological and behavioural state of the insects [32]. In the present Y-tube assays, insects consistently selected the arm containing blank microspheres rather than EO-loaded microspheres, indicating relative avoidance of the EO stimulus under the tested conditions. However, the numerical differences observed among treatments should not be interpreted as evidence that one treatment was more repellent than the others. Consequently, the treatments cannot be conclusively ranked according to repellency. Behavioural responses to plant volatiles may depend on compound identity, dose, blend composition and insect physiological condition, and the same compound may elicit attraction at lower concentrations but avoidance at higher concentrations [25,26]. The response to the tested binary mixture did not differ significantly from the responses to the individual oils. Although the EO batches were chemically characterised by GC–MS analysis, the mixture was tested at only one ratio, and the present data do not permit an assessment of additivity or synergy. This limitation is

relevant because interactions among EO constituents depend on their proportions and concentrations [33,34].

Both males and females showed consistent avoidance, suggesting that the tested stimuli can modify the behaviour of both sexes. All tested females selected the control arm in the lemongrass EO treatment; however, this observation is descriptive because the effects of sex and the treatment × sex interaction were not formally tested. Sex-dependent responses to selected plant volatiles have previously been reported in *H. halys*, including greater female sensitivity at certain concentrations of linalool oxide and nerolidol [26]. The present results therefore indicate a broadly consistent avoidance response across sexes but do not demonstrate the absence of sex-specific differences.

4.2. Encapsulation and Release Behaviour of EOs

The two oils differed in their encapsulation and release characteristics. Both calcium-alginate formulations showed high encapsulation efficiencies, exceeding 90%, indicating effective incorporation of both EOs into the alginate matrix. Lemongrass EO had higher mean encapsulation efficiency and loading capacity, whereas microspheres loaded with clove EO showed slightly greater swelling. Both formulations exhibited an initial rapid-release phase followed by a slower release phase, a biphasic pattern commonly observed in hydrogel-based delivery systems, in which compounds associated with or located near the particle surface are released relatively rapidly, followed by slower diffusion of compounds retained within the hydrated polymer network [39–41]. Such release behaviour is potentially advantageous for behaviour-modifying formulations because an initial volatile signal may be followed by a more sustained release phase.

Lemongrass EO reached near-complete cumulative release, whereas clove EO plateaued at approximately 70%. These differences may reflect oil-specific variation in chemical composition, polarity, distribution within the microspheres and interactions with the alginate matrix. GC–MS analysis confirmed that clove EO was dominated by eugenol, whereas citral, comprising geranial and neral, was the major constituent of lemongrass EO, consistent with previous studies [46,47]. Differences in the structural and physicochemical properties of these constituents, including their hydrophobicity and affinity for the polymeric matrix, may have contributed to the distinct release profiles of the two formulations. However, although the chemical composition of the tested EOs was characterised by GC–MS analysis, EO–alginate interactions were not directly investigated. Therefore, the lower release of clove EO cannot be attributed specifically to eugenol–alginate binding, and the proposed explanations remain hypotheses requiring further experimental validation. Differences in analytical recovery, stability and oil distribution may also have contributed to the observed release profiles [70,71]. Future studies combining spectroscopic and thermal characterisation of EO-loaded alginate matrices with detailed analyses of polymer–oil interactions would help clarify the mechanisms underlying the observed differences in release behaviour.

The Korsmeyer–Peppas model adequately described the initial release phase, with R^2 values above 0.97. Release exponents of 0.183 for clove EO and 0.399 for lemongrass EO were below the theoretical value of approximately 0.43 for Fickian release from spherical matrices [69,72]. The higher n value obtained for lemongrass EO suggests that its release behaviour was closer to the theoretical Fickian regime than that of clove EO. Nevertheless, the particularly low exponent for clove EO may also reflect the initial burst and heterogeneous distribution of oil within the particles. Although the Korsmeyer–Peppas parameters indicated distinct early-stage release behaviour, they should not be interpreted as definitive evidence of a particular transport mechanism because the model was fitted only to the initial portion of the release curves. Consequently, the model provides a useful empirical comparison of the two formulations but does not establish the mechanism governing EO

transport throughout the entire release period. Further mechanistic interpretation would require complementary kinetic models and structural or transport analyses.

4.3. OBP Selection and Molecular Interactions with Essential-Oil Constituents

Because OBPs participate in the peripheral recognition and transport of volatile chemical signals in the insect olfactory system, the bioinformatic analysis was used to identify an *H. halys* OBP suitable for subsequent molecular comparison with the structurally characterised DmOBP28a. Despite the generally low sequence identity among the analysed OBPs (Figure 4), their primary sequences retained the characteristic features of classical insect OBPs. In particular, the six highly conserved cysteine residues correspond to the canonical cysteine motif and are expected to form three disulfide bonds (C1–C6, C2–C5 and C3–C4), which contribute to the stabilisation of the characteristic α-helical OBP fold and the organisation of the internal ligand-binding cavity [42,43]. Thus, conservation of the cysteine pattern supports preservation of the overall OBP architecture despite substantial primary-sequence divergence.

The low median sequence identities observed within and between the HhOBP and DmOBP sets further illustrate the pronounced sequence diversity characteristic of insect OBPs. Nevertheless, phylogenetic analysis identified several groups containing proteins from both species (Figure 4). Such relationships provide a useful basis for identifying evolutionarily related proteins for comparative structural analyses. This was particularly relevant for the clade containing DmOBP19d and DmOBP28a. DmOBP28a was selected as a structural reference because its three-dimensional structure has been experimentally determined [45].

Structural comparison further supported the selection of HhOBP21. Foldseek analysis showed extensive structural similarity between HhOBP21 and DmOBP28a despite their relatively modest sequence identity, suggesting conservation of the overall compact OBP fold. In addition, DmOBP28a and HhOBP21 occupied nearby positions in the physicochemical PCA space (Figure 5). Their broadly similar physicochemical characteristics, together with their phylogenetic and structural relationships, provided complementary criteria for selecting HhOBP21 for ligand-binding analyses.

Molecular docking showed that the investigated EO constituents could be accommodated within the selected binding cavities of both HhOBP21 and DmOBP28a. Although the absolute Glide GScore values differed among the three receptor structures, the relative ranking of ligands was highly consistent (Figure 6). This agreement is notable because the binding region in the DmOBP28a crystal structure was defined by the experimentally observed pentaethylene glycol-binding site, whereas the binding sites in the AlphaFold models were identified computationally using SiteMap.

Relatively lipophilic EO constituents, particularly β-caryophyllene, α-humulene and limonene, were among the more favourably scored ligands, consistent with the role of OBPs in binding and transporting hydrophobic, poorly water-soluble odorants through the aqueous sensillar lymph. Across the three receptor structures, Glide GScore was negatively correlated with S+logP (Pearson's $r = -0.768$ to -0.687), indicating that more lipophilic ligands generally received more favourable docking scores. This pattern is consistent with an important contribution of hydrophobic interactions to ligand accommodation within the OBP binding cavities (Figures 7 and 8).

Although logP is not an explicit term in the Glide scoring function, GlideScore evaluates several contributions to protein–ligand interactions, including lipophilic contacts and van der Waals interactions, which are expected to contribute substantially to the accommodation of lipophilic ligands within the predominantly hydrophobic OBP binding cavities. Nevertheless, lipophilicity alone cannot account for the predicted binding behaviour, which

also depends on steric complementarity and other specific protein–ligand interactions. The observed GScore–S+logP relationship therefore supports a role for ligand lipophilicity in the predicted OBP–ligand interactions, while the relationship between docking scores and experimentally determined binding affinity remains to be established.

All investigated binding sites are composed mainly of hydrophobic aliphatic and aromatic amino acid residues (Figures 7 and 8). However, polar residues are also present, particularly in the pentaethylene glycol-binding site of the 6QQ4 structure, enabling hydrogen bonding with oxygen-containing functional groups of some compounds, such as the hydroxyl group of the aggregation pheromone murgantiol. The free hydroxyl group of murgantiol forms a predicted hydrogen bond with Gln28 in HhOBP21, Gly88 in the AlphaFold model of DmOBP28a, and Glu3 in the crystal structure of DmOBP28a (6QQ4).

The occurrence of favourable docking poses at different positions within the OBP cavities, as revealed by ensemble docking performed for DmOBP28a, further suggests that these proteins may accommodate chemically diverse ligands in multiple or partially overlapping binding regions. Both biologically active stereoisomers of the *H. halys* aggregation pheromone also showed favourable docking scores and therefore provided biologically relevant reference ligands for comparison with the EO constituents. However, although favourable docking scores and plausible binding poses can be used to prioritise constituents for experimental testing, they alone do not establish a direct role for the investigated OBPs in EO-mediated repellency.

Accordingly, the molecular and behavioural results should be interpreted as complementary rather than directly causal. Molecular docking provides evidence of structural compatibility between selected EO constituents and the investigated OBP cavities, whereas the Y-tube experiments demonstrate that the complete EO formulations elicit avoidance at the behavioural level. Experimental ligand-binding assays would be required to validate the predicted OBP–ligand interactions, while subsequent receptor-level and neurophysiological studies would be needed to determine how molecular recognition translates into attraction or repellency. Molecular dynamics simulations could also help evaluate the stability of the predicted complexes and the flexibility of the OBP binding cavities.

4.4. Predicted Ecotoxicity, Environmental Fate and Study Limitations

The predicted ecotoxicological profiles provided additional environmental pre-screening of the selected constituents of clove and lemongrass EOs (Figure 9). For all investigated compounds, the predicted acute-toxicity values for the aquatic model organisms *Daphnia magna*, *Tetrahymena pyriformis* and *Pimephales promelas* remained below the applied classification thresholds. These results therefore indicate a generally favourable predicted acute-toxicity profile for the evaluated aquatic test organisms under the classification criteria applied in this study.

Predicted environmental fate showed greater variation among the constituents. Bioconcn values exceeding the applied threshold were predicted for six EO constituents: β-caryophyllene, α-humulene, limonene, methyl eugenol, linalool and geraniol. Five of these are constituents of clove EO, while limonene and geraniol are present in lemongrass EO. β-Caryophyllene, α-humulene and methyl eugenol were also predicted not to be readily biodegradable. The major components of the studied EOs, eugenol and citral, were predicted to have low acute toxicity and bioaccumulation potential and to be readily biodegradable.

Predicted acute-toxicity values below the applied thresholds do not exclude environmental concerns associated with persistence or bioaccumulation. The higher lipophilicity of several of these constituents may contribute to their predicted bioaccumulation potential. These predictions further emphasise that the plant origin of EOs should not, by itself, be taken as evidence of environmental safety [28,71]. Thus, the predicted acute-toxicity, bio-

concentration and biodegradability data should be considered complementary components of an initial environmental hazard assessment, while a comprehensive evaluation of environmental safety would require experimental ecotoxicity, bioaccumulation, and environmental fate studies.

Several limitations directly affect the interpretation of the present findings. Behavioural assays across a broader range of EO concentrations and mixture ratios are needed to define dose-dependent responses; therefore, the present data do not establish an optimal concentration or mixture composition. Because insects within each replicate were tested simultaneously, their choices may not have been fully independent; this should be considered when interpreting the pooled percentages and associated statistical results. Experimental ligand-binding and toxicity assays are needed to validate in silico predictions. Without experimental ligand-binding data, the docking results cannot establish that HhOBP21 binds the investigated constituents under biological conditions or mediates the observed behavioural response. Likewise, the predicted ecotoxicity and environmental-fate profiles cannot be taken as evidence of environmental safety. Nevertheless, computational approaches provide relatively rapid and cost-effective tools for generating preliminary insights into molecular interactions and toxicity-related properties of compounds, such as the EO constituents investigated in the present study, and for developing hypotheses for subsequent experimental testing. Similarly, the behavioural assays performed in this study provide evidence of avoidance under the investigated experimental conditions, while further dose–response studies are needed to establish the concentration dependence and robustness of these effects.

Finally, semi-field and field studies are needed to determine whether the olfactory avoidance observed in the Y-tube translates into spatial repellency and reduced *H. halys* presence or crop injury under agricultural conditions. The performance of the encapsulated formulations under these conditions remains to be tested.

5. Conclusions

Clove leaf and lemongrass essential-oil formulations induced strong avoidance responses in adult *H. halys*, with no significant differences detected among the individual oils and their binary combination. Combined phylogenetic, structural, and physicochemical analyses supported the putative function of HhOBP21 as an OBP, and HhOBP21 was therefore selected for subsequent molecular modelling together with the reference protein DmOBP28a. Molecular docking indicated that constituents of both oils are structurally compatible with the binding cavities of HhOBP21 and the reference DmOBP28a, suggesting potential interactions with these OBPs that require experimental validation. Both EOs were successfully incorporated into calcium-alginate microspheres with encapsulation efficiencies above 90%, while their distinct release profiles demonstrated oil-specific differences in formulation and release behaviour. Predicted ecotoxicological profiles indicated acute-toxicity values below the applied thresholds for the evaluated aquatic organisms but identified potential concerns related to the bioaccumulation and biodegradability of several constituents.

Overall, the integration of behavioural, formulation and molecular results supports further semi-field and field evaluation of clove and lemongrass EOs and their formulations to determine whether the laboratory olfactory avoidance observed in this study translates into effective spatial repellency under agricultural conditions.

Supplementary Materials: The following supporting information can be downloaded at: https://www.mdpi.com/article/10.3390/agriculture16212385/s1. File S1: GC–MS spectra and compositional analysis of the clove leaf and lemongrass essential oils used in this study.

Author Contributions: Conceptualization, I.P.Ž. and D.L., and V.S. for in silico part; methodology, I.P.Ž., D.L., M.P.B., H.V.G., M.V., K.V.-K., P.T. and V.S.; validation, I.P.Ž., D.L., M.V., K.V.-K., P.T. and V.S.; formal analysis, I.P.Ž., D.L., M.V., K.V.-K., P.T. and V.S.; investigation, M.P.B., H.V.G., I.P.Ž., D.L., K.V.-K. and P.T.; resources, I.P.Ž., D.L., H.V.G. and V.S.; data curation, M.P.B., H.V.G., I.P.Ž., D.L., M.V., K.V.-K., P.T. and V.S.; writing—original draft preparation, I.P.Ž., D.L., M.V. and V.S.; writing—review and editing, I.P.Ž., M.P.B., H.V.G., M.V., K.V.-K., P.T., V.S. and D.L.; visualization, I.P.Ž., D.L., H.V.G., M.V. and V.S.; supervision, I.P.Ž. and D.L.; project administration, I.P.Ž. and D.L.; funding acquisition, D.L. and V.S. All authors have read and agreed to the published version of the manuscript.

Funding: This study was supported by the Croatian Science Foundation (project LAIDYGRID, IP-2025-02-7105) and partially funded by the University of Zagreb Faculty of Agriculture through the institutional project DEMO IPM (project number AGR_05). V. Stepanić gratefully acknowledges the Simulations Plus University+ (formerly SLP Academic) Program for granting access to ADMET Predictor™.

Institutional Review Board Statement: Not applicable.

Data Availability Statement: The original contributions presented in this study are included in the article. Further inquiries can be directed to the corresponding authors.

Acknowledgments: During the preparation of this manuscript, the authors used ChatGPT (GPT-6; OpenAI, San Francisco, CA, USA) for language editing and assistance with the preparation of Figure 3, Figure 9 and the graphical abstract based exclusively on data generated by the authors during the study. ChatGPT was not used to generate, modify, analyse, or infer research data. The authors reviewed and edited all AI-assisted output and take full responsibility for the content of this publication.

Conflicts of Interest: The authors declare no conflicts of interest.

Abbreviations

The following abbreviations are used in this manuscript:

ADMET	Absorption, distribution, metabolism, excretion, and toxicity
ANN	Artificial neural network
BCF	Bioconcentration factor
DmOBP	*Drosophila melanogaster* odorant-binding protein
EE	Encapsulation efficiency
EO	Essential oil
GRAVY	Grand average of hydropathicity
HhOBP	*Halyomorpha halys* odorant-binding protein
KP	Korsmeyer–Peppas
LC	Loading capacity
MFP	ModelFinder Plus
MSA	Multiple sequence alignment
MW	Molecular weight
OBP	Odorant-binding protein
PCA	Principal component analysis
PDB	Protein Data Bank
pI	Isoelectric point
PTFE	Polytetrafluoroethylene
RI	Repellency index
SDS	Safety data sheet
SMILES	Simplified Molecular Input Line Entry System
SP	Standard precision
Sw	Swelling degree
UV/VIS	Ultraviolet–visible

References

1. Lee, D.-H.; Short, B.D.; Joseph, S.V.; Bergh, J.C.; Leskey, T.C. Review of the Biology, Ecology, and Management of *Halyomorpha halys* (Hemiptera: Pentatomidae) in China, Japan, and the Republic of Korea. *Environ. Entomol.* **2013**, *42*, 627–641. [CrossRef]
2. Leskey, T.C.; Nielsen, A.L. Impact of the Invasive Brown Marmorated Stink Bug in North America and Europe: History, Biology, Ecology, and Management. *Annu. Rev. Entomol.* **2018**, *63*, 599–618. [CrossRef]
3. Pajač Beus, M.; Lemić, D.; Skendžić, S.; Čirjak, D.; Pajač Živković, I. The Brown Marmorated Stink Bug (Hemiptera: Pentatomidae)—A Major Challenge for Global Plant Production. *Agriculture* **2024**, *14*, 1322. [CrossRef]
4. Rice, K.B.; Bergh, C.J.; Bergmann, E.J.; Biddinger, D.J.; Dieckhoff, C.; Dively, G.; Fraser, H.; Gariepy, T.; Hamilton, G.; Haye, T.; et al. Biology, ecology and management of brown marmorated stink bug (Hemiptera: Pentatomidae). *J. Integr. Pest Manag.* **2014**, *5*, A1–A13. [CrossRef]
5. Pajač Živković, I.; Skendžić, S.; Lemić, D. Rapid spread and first massive occurrence of *Halyomorpha halys* (Stål, 1855) in agricultural production in Croatia. *J. Cent. Eur. Agric.* **2021**, *22*, 531–538. [CrossRef]
6. Pajač Živković, I.; Čirjak, D.; Miklečić, I.; Pintar, M.; Duralija, B.; Lemić, D. First Evidence of the Brown Marmorated Stink Bug and Its Population Size in Perennial Crops in Croatia. *J. Cent. Eur. Agric.* **2023**, *24*, 908–915. [CrossRef]
7. Berteloot, O.H.; Peusens, G.; Beliën, T.; De Clercq, P.; Van Leeuwen, T. Unveiling the Diet of Two Generalist Stink Bugs, *Halyomorpha halys* and *Pentatoma rufipes* (Hemiptera: Pentatomidae), through Metabarcoding of the ITS2 Region from Gut Content. *Pest Manag. Sci.* **2024**, *80*, 5694–5705. [CrossRef]
8. Hadden, W.T.; Hepler, J.R.; Beers, E.H.; Cooper, W.R.; Leskey, T.C.; Bergh, J.C. Characterizing brown marmorated stink bug, *Halyomorpha halys* Stål, host plant usage and acceptability: Methodological strengths and shortcomings. *Entomol. Exp. Appl.* **2025**, *173*, 403–416. [CrossRef]
9. Bakken, A.J.; Schoof, S.C.; Bickerton, M.; Kamminga, K.L.; Jenrette, J.C.; Malone, S.; Abney, M.A.; Herbert, D.A.; Reisig, D.; Kuhar, T.P.; et al. Occurrence of Brown Marmorated Stink Bug (Hemiptera: Pentatomidae) on Wild Hosts in Nonmanaged Woodlands and Soybean Fields in North Carolina and Virginia. *Environ. Entomol.* **2015**, *44*, 1011–1021. [CrossRef]
10. Park, Y.-L.; Choi, K.; Cullum, J.; Hoelmer, K.A.; Weber, D.C.; Morrison, W.R., III; Rice, K.B.; Krawczyk, G.; Fleischer, S.J.; Hamilton, G.; et al. Landscape-Scale Spatiotemporal Dynamics of *Halyomorpha halys* (Stål) (Hemiptera: Pentatomidae) Populations: Implications for Spatially-Based Pest Management. *Pest Manag. Sci.* **2024**, *80*, 953–966. [CrossRef]
11. Pajač Beus, M.; Pajač Živković, I.; Skendrović Babojelić, M.; Maršić, N.; Lemic, D. Cultivar-Dependent Expression of *Halyomorpha halys* Impact in a Commercial Apple Orchard: Implications for Integrated Pest Management. *Agriculture* **2026**, *16*, 627. [CrossRef]
12. Joseph, S.V.; Nita, M.; Leskey, T.C.; Bergh, J.C. Temporal Effects on the Incidence and Severity of Brown Marmorated Stink Bug (Hemiptera: Pentatomidae) Feeding Injury to Peaches and Apples during the Fruiting Period in Virginia. *J. Econ. Entomol.* **2015**, *108*, 592–599. [CrossRef]
13. Leskey, T.C.; Lee, D.-H.; Short, B.D.; Wright, S.E. Impact of Insecticides on the Invasive *Halyomorpha halys* (Hemiptera: Pentatomidae): Analysis of Insecticide Lethality. *J. Econ. Entomol.* **2012**, *105*, 1726–1735. [CrossRef]
14. Leskey, T.C.; Short, B.D.; Butler, B.R.; Wright, S.E. Impact of the Invasive Brown Marmorated Stink Bug, *Halyomorpha halys* (Stål), in Mid-Atlantic Tree Fruit Orchards in the United States: Case Studies of Commercial Management. *Psyche J. Entomol.* **2012**, *2012*, 535062. [CrossRef]
15. Leskey, T.C.; Short, B.D.; Lee, D.-H. Efficacy of Insecticide Residues on Adult *Halyomorpha halys* (Stål) (Hemiptera: Pentatomidae) Mortality and Injury in Apple and Peach Orchards. *Pest Manag. Sci.* **2014**, *70*, 1097–1104. [CrossRef]
16. Ogburn, E.C.; Walgenbach, J.F. Effects of Insecticides Used in Organic Agriculture on *Anastatus reduvii* (Hymenoptera: Eupelmidae) and *Telenomus podisi* (Hymenoptera: Scelionidae), Egg Parasitoids of Pestivorous Stink Bugs. *J. Econ. Entomol.* **2019**, *112*, 108–114. [CrossRef]
17. Ribeiro, A.V.; Holle, S.G.; Hutchison, W.D.; Koch, R.L. Lethal and Sublethal Effects of Conventional and Organic Insecticides on the Parasitoid *Trissolcus japonicus*, a Biological Control Agent for *Halyomorpha halys*. *Front. Insect Sci.* **2021**, *1*, 685755. [CrossRef]
18. Candian, V.; Pansa, M.G.; Briano, R.; Peano, C.; Tedeschi, R.; Tavella, L. Exclusion Nets: A Promising Tool to Prevent *Halyomorpha halys* from Damaging Nectarines and Apples in NW Italy. *Bull. Insectol.* **2018**, *71*, 21–30.
19. Fornasiero, D.; Scaccini, D.; Lombardo, V.; Galli, G.; Pozzebon, A. Effect of Exclusion Net Timing of Deployment and Color on *Halyomorpha halys* (Hemiptera: Pentatomidae) Infestation in Pear and Apple Orchards. *Crop Prot.* **2023**, *172*, 106331. [CrossRef]
20. Morrison, W.R., III; Lee, D.-H.; Short, B.D.; Khrimian, A.; Leskey, T.C. Establishing the Behavioral Basis for an Attract-and-Kill Strategy to Manage the Invasive *Halyomorpha halys* in Apple Orchards. *J. Pest Sci.* **2016**, *89*, 81–96. [CrossRef]
21. Masetti, A.; Morelli, A.; Fagioli, L.; Pradolesi, G.; Nicoli, R.; Scagliarini, O.; Tommasini, M.G.; Preti, M. Evaluation of an Attract-and-Kill Strategy Using Long-Lasting Insecticide Nets for the Management of the Brown Marmorated Stink Bug in Northern Italy. *Insects* **2024**, *15*, 577. [CrossRef]
22. Ioriatti, C.; Mazzoni, V.; Franceschi, P.; Chiesa, S.G.; Angeli, G.; De Concini, M.; Panizza, C.; Martini, F.; Zapponi, L.; Anfora, G. Classical Biological Control of the Brown Marmorated Stink Bug (*Halyomorpha halys*) in Apple Orchard: A Success Story. *Pest Manag. Sci.* **2025**, *81*, 8500–8509. [CrossRef]

23. Chierici, E.; Marchetti, E.; Poccia, A.; Russo, A.; Giannuzzi, V.A.; Governatori, L.; Zucchi, L.; Rondoni, G.; Conti, E. Laboratory and Field Efficacy of Natural Products against the Invasive Pest *Halyomorpha halys* and Side Effects on the Biocontrol Agent *Trissolcus japonicus*. *Sci. Rep.* **2025**, *15*, 4622. [CrossRef]
24. Weber, D.C.; Leskey, T.C.; Cabrera Walsh, G.; Khrimian, A. Synergy of Aggregation Pheromone with Methyl (E,E,Z)-2,4,6-Decatrienoate in Attraction of *Halyomorpha halys* (Hemiptera: Pentatomidae). *J. Econ. Entomol.* **2014**, *107*, 1061–1068. [CrossRef]
25. Akotsen-Mensah, C.; Blaauw, B.R.; Rivera, M.J.; Rodriguez-Saona, C.; Nielsen, A.L. Behavioral Response of *Halyomorpha halys* (Hemiptera: Pentatomidae) and Its Egg Parasitoid *Trissolcus japonicus* (Hymenoptera: Scelionidae) to Host Plant Odors. *Front. Ecol. Evol.* **2021**, *9*, 696814. [CrossRef]
26. Zhong, Y.-Z.; Xie, M.-H.; Huang, C.; Zhang, X.; Cao, L.; Chen, H.-L.; Zhang, F.; Wan, F.-H.; Han, R.-C.; Tang, R. Characterizations of botanical attractant of *Halyomorpha halys* and selection of relevant deorphanization candidates via computational approach. *Sci. Rep.* **2022**, *12*, 4170. [CrossRef]
27. Burt, S.A. Essential Oils: Their Antibacterial Properties and Potential Applications in Foods—A Review. *Int. J. Food Microbiol.* **2004**, *94*, 223–253. [CrossRef]
28. Regnault-Roger, C.; Vincent, C.; Arnason, J.T. Essential Oils in Insect Control: Low-Risk Products in a High-Stakes World. *Annu. Rev. Entomol.* **2012**, *57*, 405–424. [CrossRef]
29. Isman, M.B. Botanical Insecticides, Deterrents, and Repellents in Modern Agriculture and an Increasingly Regulated World. *Annu. Rev. Entomol.* **2006**, *51*, 45–66. [CrossRef]
30. Turek, C.; Stintzing, F.C. Stability of Essential Oils: A Review. *Compr. Rev. Food Sci. Food Saf.* **2013**, *12*, 40–53. [CrossRef]
31. Zhang, Q.-H.; Schneidmiller, R.G.; Hoover, D.R.; Zhou, G.; Margaryan, A.; Bryant, P. Essential Oils as Spatial Repellents for the Brown Marmorated Stink Bug, *Halyomorpha halys* (Stål) (Hemiptera: Pentatomidae). *J. Appl. Entomol.* **2014**, *138*, 490–499. [CrossRef]
32. Bulgarini, G.; Bortolini, S.; Maistrello, L. Repellent Activity of Essential Oils on Adults of *Halyomorpha halys* (Heteroptera: Pentatomidae) in Different Physiological-Behavioural Phases. *J. Appl. Entomol.* **2021**, *145*, 575–586. [CrossRef]
33. Noosidum, A.; Chareonviriyaphap, T.; Chandrapatya, A. Synergistic Repellent and Irritant Effect of Combined Essential Oils on *Aedes aegypti* (L.) *Mosquitoes*. *J. Vector Ecol.* **2014**, *39*, 298–305. [CrossRef]
34. Nararak, J.; Sanguanpong, U.; Sukkanon, C.; Manguin, S.; Chareonviriyaphap, T. Synergistic Repellent and Irritant Effects of a Mixture of β-Caryophyllene Oxide and Vetiver Oil against Mosquito Vectors. *Insects* **2023**, *14*, 773. [CrossRef]
35. Donsì, F.; Ferrari, G. Essential Oil Nanoemulsions as Antimicrobial Agents in Food. *J. Biotechnol.* **2016**, *233*, 106–120. [CrossRef]
36. Hyldgaard, M.; Mygind, T.; Meyer, R.L. Essential Oils in Food Preservation: Mode of Action, Synergies, and Interactions with Food Matrix Components. *Front. Microbiol.* **2012**, *3*, 12. [CrossRef]
37. Solomon, B.; Sahle, F.F.; Gebre-Mariam, T.; Asres, K.; Neubert, R.H.H. Microencapsulation of Citronella Oil for Mosquito-Repellent Application: Formulation and In Vitro Permeation Studies. *Eur. J. Pharm. Biopharm.* **2012**, *80*, 61–66. [CrossRef]
38. Hogenbom, J.; Jones, A.; Wang, H.V.; Pickett, L.J.; Faraone, N. Synthesis and Characterization of β-Cyclodextrin–Essential Oil Inclusion Complexes for Tick Repellent Development. *Polymers* **2021**, *13*, 1892. [CrossRef]
39. George, M.; Abraham, T.E. Polyionic Hydrocolloids for the Intestinal Delivery of Protein Drugs: Alginate and Chitosan—A Review. *J. Control. Release* **2006**, *114*, 1–14. [CrossRef]
40. Lee, K.Y.; Mooney, D.J. Alginate: Properties and Biomedical Applications. *Prog. Polym. Sci.* **2012**, *37*, 106–126. [CrossRef]
41. Draget, K.I.; Skjåk-Bræk, G.; Smidsrød, O. Alginate Based New Materials. *Int. J. Biol. Macromol.* **1997**, *21*, 47–55. [CrossRef]
42. Rihani, K.; Ferveur, J.-F.; Briand, L. The 40-Year Mystery of Insect Odorant-Binding Proteins. *Biomolecules* **2021**, *11*, 509. [CrossRef]
43. Shukla, S.; Nakano-Baker, O.; Godin, D.; MacKenzie, D.; Sarikaya, M. iOBPdb: A Database for Experimentally Determined Functional Characterization of Insect Odorant Binding Proteins. *Sci. Data* **2023**, *10*, 295. [CrossRef]
44. Gouda, M.N.R.; Subramanian, S. Odorant-binding proteins and chemosensory proteins in insects: Structural insights, functional plasticity, and prospects for targeted pest management. *Mol. Biol. Rep.* **2026**, *53*, 787. [CrossRef]
45. Gonzalez, D.; Rihani, K.; Neiers, F.; Poirier, N.; Fraichard, S.; Gotthard, G.; Chertemps, T.; Maïbèche, M.; Ferveur, J.-F.; Briand, L. The *Drosophila* Odorant-Binding Protein 28a Is Involved in the Detection of the Floral Odour β-Ionone. *Cell. Mol. Life Sci.* **2020**, *77*, 2565–2577. [CrossRef]
46. Haro-González, J.N.; Castillo-Herrera, G.A.; Martínez-Velázquez, M.; Espinosa-Andrews, H. Clove Essential Oil (*Syzygium aromaticum* L. Myrtaceae): Extraction, Chemical Composition, Food Applications, and Essential Bioactivity for Human Health. *Molecules* **2021**, *26*, 6387. [CrossRef]
47. Luang-In, V.; Saengha, W.; Karirat, T.; Senakun, C.; Siriamornpun, S. Phytochemical Profile of Cymbopogon citratus (DC.) Stapf Lemongrass Essential Oil from Northeastern Thailand and Its Antioxidant and Antimicrobial Attributes and Cytotoxic Effects on HT-29 Human Colorectal Adenocarcinoma Cells. *Foods* **2024**, *13*, 2928. [CrossRef]
48. Vinceković, M.; Jalšenjak, N.; Topolovec-Pintarić, S.; Đermić, E.; Bujan, M.; Jurić, S. Encapsulation of Biological and Chemical Agents for Plant Nutrition and Protection: Chitosan/Alginate Microcapsules Loaded with Copper Cations and *Trichoderma viride*. *J. Agric. Food Chem.* **2016**, *64*, 8073–8083. [CrossRef]

49. Vinceković, M.; Živković, L.; Turkeyeva, E.; Mutaliyeva, B.; Madybekova, G.; Šegota, S.; Šijaković Vujičić, N.; Pustak, A.; Jurkin, T.; Kiš, M.; et al. Development of Alginate Composite Microparticles for Encapsulation of *Bifidobacterium animalis* subsp. *lactis*. *Gels* **2024**, *10*, 752. [CrossRef]
50. Gylling Data Management Inc. *ARM 2025® GDM Software*, revision 2025.2 (16 October 2025); Gylling Data Management Inc.: Brookings, SD, USA, 2025.
51. Kim, S.; Chen, J.; Cheng, T.; Gindulyte, A.; He, J.; He, S.; Li, Q.; Shoemaker, B.A.; Thiessen, P.A.; Yu, B.; et al. PubChem 2023 Update. *Nucleic Acids Res*. **2023**, *51*, D1373–D1380. [CrossRef]
52. Schrödinger, LLC. *Schrödinger Release 2026-2*; Schrödinger, LLC: New York, NY, USA, 2026.
53. Khrimian, A.; Zhang, A.; Weber, D.C.; Ho, H.-Y.; Aldrich, J.R.; Vermillion, K.E.; Siegler, M.A.; Shirali, S.; Guzman, F.; Leskey, T.C. Discovery of the Aggregation Pheromone of the Brown Marmorated Stink Bug (*Halyomorpha halys*) through the Creation of Stereoisomeric Libraries of 1-Bisabolen-3-ols. *J. Nat. Prod*. **2014**, *77*, 1708–1717. [CrossRef]
54. The UniProt Consortium. UniProt: The Universal Protein Knowledgebase in 2025. *Nucleic Acids Res*. **2025**, *53*, D609–D617. [CrossRef]
55. Jumper, J.; Evans, R.; Pritzel, A.; Green, T.; Figurnov, M.; Ronneberger, O.; Tunyasuvunakool, K.; Bates, R.; Žídek, A.; Potapenko, A.; et al. Highly accurate protein structure prediction with AlphaFold. *Nature* **2021**, *596*, 583–589. [CrossRef]
56. Varadi, M.; Bertoni, D.; Magana, P.; Paramval, U.; Pidruchna, I.; Radhakrishnan, M.; Tsenkov, M.; Nair, S.; Mirdita, M.; Yeo, J.; et al. AlphaFold Protein Structure Database in 2024: Providing structure coverage for over 214 million protein sequences. *Nucleic Acids Res*. **2024**, *52*, D368–D375. [CrossRef]
57. Tamura, K.; Stecher, G.; Kumar, S. MEGA11: Molecular Evolutionary Genetics Analysis Version 11. *Mol. Biol. Evol*. **2021**, *38*, 3022–3027. [CrossRef]
58. Waterhouse, A.M.; Procter, J.B.; Martin, D.M.A.; Clamp, M.; Barton, G.J. Jalview Version 2—A multiple sequence alignment editor and analysis workbench. *Bioinformatics* **2009**, *25*, 1189–1191. [CrossRef]
59. Nguyen, L.-T.; Schmidt, H.A.; von Haeseler, A.; Minh, B.Q. IQ-TREE: A fast and effective stochastic algorithm for estimating maximum-likelihood phylogenies. *Mol. Biol. Evol*. **2015**, *32*, 268–274. [CrossRef]
60. Kalyaanamoorthy, S.; Minh, B.Q.; Wong, T.K.F.; von Haeseler, A.; Jermiin, L.S. ModelFinder: Fast Model Selection for Accurate Phylogenetic Estimates. *Nat. Methods* **2017**, *14*, 587–589. [CrossRef]
61. Hoang, D.T.; Chernomor, O.; von Haeseler, A.; Minh, B.Q.; Vinh, L.S. UFBoot2: Improving the Ultrafast Bootstrap Approximation. *Mol. Biol. Evol*. **2018**, *35*, 518–522. [CrossRef]
62. Rambaut, A. *FigTree*, version 1.4.4; Institute of Evolutionary Biology, University of Edinburgh: Edinburgh, UK, 2018.
63. van Kempen, M.; Kim, S.S.; Tumescheit, C.; Mirdita, M.; Lee, J.; Gilchrist, C.L.M.; Söding, J.; Steinegger, M. Fast and Accurate Protein Structure Search with Foldseek. *Nat. Biotechnol*. **2024**, *42*, 243–246. [CrossRef]
64. Cock, P.J.A.; Antao, T.; Chang, J.T.; Chapman, B.A.; Cox, C.J.; Dalke, A.; Friedberg, I.; Hamelryck, T.; Kauff, F.; Wilczynski, B.; et al. Biopython: Freely Available Python Tools for Computational Molecular Biology and Bioinformatics. *Bioinformatics* **2009**, *25*, 1422–1423. [CrossRef]
65. Sander, T.; Freyss, J.; von Korff, M.; Rufener, C. DataWarrior: An Open-Source Program for Chemistry Aware Data Visualization and Analysis. *J. Chem. Inf. Model*. **2015**, *55*, 460–473. [CrossRef]
66. Halgren, T.A. Identifying and characterizing binding sites and assessing druggability. *J. Chem. Inf. Model*. **2009**, *49*, 377–389. [CrossRef]
67. Ghosh, J.; Lawless, M.S.; Waldman, M.; Gombar, V.K.; Fraczkiewicz, R. Modeling ADMET. In *In Silico Methods for Predicting Drug Toxicity*; Methods in Molecular Biology; Humana Press: New York, NY, USA, 2016; Volume 1425, pp. 63–83. [CrossRef]
68. Pehar, V.; Kolić, D.; Zandona, A.; Šinko, G.; Katalinić, M.; Stepanić, V.; Kovarik, Z. Selected Herbicides Screened for Toxicity and Analysed as Inhibitors of Both Cholinesterases. *Chem. Biol. Interact*. **2023**, *379*, 110506. [CrossRef]
69. Korsmeyer, R.W.; Gurny, R.; Doelker, E.; Buri, P.; Peppas, N.A. Mechanisms of Solute Release from Porous Hydrophilic Polymers. *Int. J. Pharm*. **1983**, *15*, 25–35. [CrossRef]
70. Salvia-Trujillo, L.; Rojas-Graü, A.; Soliva-Fortuny, R.; Martín-Belloso, O. Physicochemical Characterization and Antimicrobial Activity of Food-Grade Emulsions and Nanoemulsions Incorporating Essential Oils. *Food Hydrocoll*. **2015**, *43*, 547–556. [CrossRef]
71. Ayllón-Gutiérrez, R.; Díaz-Rubio, L.; Montaño-Soto, M.; Haro-Vázquez, M.d.P.; Córdova-Guerrero, I. Applications of Plant Essential Oils in Pest Control and Their Encapsulation for Controlled Release: A Review. *Agriculture* **2024**, *14*, 1766. [CrossRef]
72. Ritger, P.L.; Peppas, N.A. A Simple Equation for Description of Solute Release I. Fickian and Non-Fickian Release from Non-Swellable Devices in the Form of Slabs, Spheres, Cylinders or Discs. *J. Control. Release* **1987**, *5*, 23–36. [CrossRef]

Disclaimer/Publisher's Note: The statements, opinions and data contained in all publications are solely those of the individual author(s) and contributor(s) and not of MDPI and/or the editor(s). MDPI and/or the editor(s) disclaim responsibility for any injury to people or property resulting from any ideas, methods, instructions or products referred to in the content.